PHARMACOEPIDEMIOLOGY AND DRUG SAFETY (2014)
Published online in Wiley Online Library (wileyonlinelibrary.com) **DOI**: 10.1002/pds.3603

BRIEF REPORT

A detection algorithm for drug-induced liver injury in medical information databases using the Japanese diagnostic scale and its comparison with the Council for International Organizations of Medical Sciences/the Roussel Uclaf Causality Assessment Method scale

Tadaaki Hanatani[1,2], Kimie Sai[1]*, Masahiro Tohkin[2], Katsunori Segawa[1], Michio Kimura[3], Katsuhito Hori[4], Junichi Kawakami[4] and Yoshiro Saito[1]

[1]*Division of Medicinal Safety Science, National Institute of Health Sciences, Tokyo, Japan*
[2]*Department of Regulatory Science, Graduate School of Pharmaceutical Sciences, Nagoya City University, Aichi, Japan*
[3]*Department of Medical Informatics, Hamamatsu University School of Medicine, Shizuoka, Japan*
[4]*Department of Hospital Pharmacy, Hamamatsu University School of Medicine, Shizuoka, Japan*

ABSTRACT

Purpose Drug-induced liver injury (DILI) is one of the primary targets for pharmacovigilance using medical information databases (MIDs). Because of diagnostic complexity, a standardized method for identifying DILI using MIDs has not yet been established. We applied the Digestive Disease Week Japan 2004 (DDW-J) scale, a Japanese clinical diagnostic criteria for DILI, to a DILI detection algorithm, and compared it with the Council for International Organizations of Medical Sciences/the Roussel Uclaf Causality Assessment Method (CIOMS/RUCAM) scale to confirm its consistency. Characteristics of DILI cases identified by the DDW-J algorithm were examined in two Japanese MIDs.

Methods Using an MID from the Hamamatsu University Hospital, we constructed a DILI detection algorithm on the basis of the DDW-J scale. We then compared the findings between the DDW-J and CIOMS/RUCAM scales. We examined the characteristics of DILI after antibiotic treatment in the Hamamatsu population and a second population that included data from 124 hospitals, which was derived from an MID from the Medical Data Vision Co., Ltd. We performed a multivariate logistic regression analysis to assess the possible DILI risk factors.

Results The concordance rate was 79.4% between DILI patients identified by the DDW-J and CIOMS/RUCAM; the Spearman rank correlation coefficient was 0.952 ($P < 0.0001$). Men showed a significantly higher risk for DILI after antibiotic treatments in both MID populations.

Conclusions The DDW-J and CIOMS/RUCAM algorithms were equivalent for identifying the DILI cases, confirming the utility of our DILI detection method using MIDs. This study provides evidence supporting the use of MID analyses to improve pharmacovigilance.

KEY WORDS—drug-induced liver injury; medical information database; pharmacovigilance; DDW-J; antibiotics; pharmacoepidemiology

Received 31 July 2013; Revised 20 January 2014; Accepted 29 January 2014

INTRODUCTION

Drug-induced liver injury (DILI) is a clinically problematic issue and a major cause of acute liver failure.[1–3] In general, DILI diagnosis is complex and nonstandardized because of the difficulty in detection and lack of reliable markers.[4,5] Therefore, clinical scales were developed to facilitate DILI diagnosis. The Council for International Organizations of Medical Sciences/the Roussel Uclaf Causality Assessment Method (CIOMS/RUCAM) scale was proposed[6] and has been generally used as a standardized diagnostic tool. In Japan, the Digestive Disease Week Japan 2004 (DDW-J) scale, which is highly sensitive (92.1%) and specific (88.1%), was developed by modifying the CIOMS/RUCAM scale.[7,8] In particular, the factor of co-medication was excluded, and the factors of drug lymphocyte stimulation test and eosinophilia were included according to Japan's clinical environment.

*Correspondence to: K. Sai, Division of Medicinal Safety Science, National Institute of Health Sciences, Kamiyoga 1-18-1, Setagaya-ku, Tokyo 158-8501, Japan. Email: sai@nihs.go.jp

Challenges using medical information databases (MIDs) for identifying DILI have been addressed worldwide,[9,10] but a standardized method for such analyses has not yet been established. Because a diagnosis scale based on numerical or quantitative information was considered suitable for MID-based research, we constructed a detection algorithm for DILI on the basis of the DDW-J scale.

METHODS

Data source and ethics

This study was performed using two data sources: one was a high-speed retrieval system at the Hamamatsu University Hospital (Shizuoka, Japan),[11] and the other was a commercial MID developed by the Medical Data Vision Co., Ltd. (MDV, Tokyo, Japan) that contained data from 124 large and mainly tertiary hospitals in Japan. The mean follow-up period within this MID was 243 days. MIDs from Hamamatsu and MDV included health records from approximately 200 000 and 4 400 000 patients, respectively. The two MIDs had similar age structures. We used only anonymized data in our analysis. This study was approved by the ethics committees of both the Hamamatsu University School of Medicine and the National Institute of Health Sciences.

Study population

Clarithromycin (CM), azithromycin (AM), levofloxacin (LX), and moxifloxacin (MX) for internal use were examined in this study because of their similar clinical indications and their wide use in Japan. The subject inclusion criteria were as follows: (i) received at least one prescription for one of the study drugs between 1 April 2007 and 31 March 2012 in the Hamamatsu MID and between 1 April 2008 and 31 August 2011 in the MDV MID; (ii) no other study drug prescription between 90 days prior to the index date (the first day of the study drug administration) and the last administration in the first prescription term (>180-day interval between the study drug administrations); (iii) 18 years old or older at the index date; (iv) received alanine aminotransferase, and alkaline phosphatase tests in the preceding period (within 90 days prior to the index date) and the follow-up period (within 180 days after the last administration); (v) no occurrence of liver injury (alanine aminotransferase $> 2 \times$ the upper limit of normal value or alkaline phosphatase > upper limit of normal value) in the preceding period; (vi) no medical history in the preceding period of HIV (B20-24) or cancer (C00-97) as determined by the International Statistical Classification of Diseases and Related Health Problems, 10th revision.

Characteristics

On the basis of the general considerations for usage and dosage in each label, a long treatment was considered ≥8 days with CM, LX, and MX and ≥4 days with AM; a high dose was considered an average daily dose of >400 mg/day for CM and MX, >500 mg/day for AM and LX, and >2000 mg/day for AM in dry syrup form for single administration.

Algorithm for identifying drug-induced liver injury

We applied the original DDW-J scoring to the DILI detection algorithm consistently.[12] In addition, the algorithm based on the CIOMS/RUCAM scale was used as a reference.[6] Details regarding these two scales are summarized in Table S1. According to the definition of each scale, DILI was defined as a total score ≥5 in the DDW-J and ≥6 in the CIOMS/RUCAM algorithm.

Statistical analysis

To calculate the odds ratios (ORs) for DILI onset and those between DILI and non-DILI groups, we performed a multivariate logistic regression analysis adjusting for age (≥55 years), gender, in/outpatient status, diabetes mellitus, treatment duration, and high dose. Values of $P < 0.05$ (two-sided) were considered statistically significant. All statistical analyses were conducted using SAS software, version 9.3 (SAS Institute Inc., NC, USA).

RESULTS

Assessment of drug-induced liver injury detection algorithm

Using the DDW-J algorithm in the Hamamatsu population, we detected 182 DILI patients. To assess the utility of the DDW-J algorithm, we compared the results with those obtained with the CIOMS/RUCAM algorithm. Because the CIOMS/RUCAM scale excludes the delayed onset cases (>15 days for hepatocellular type or >30 days for cholestatic or mixed type after stopping the drug) from scoring except when dealing with slowly metabolized chemicals, the comparison was performed in the nondelayed onset population (Figure 1). The concordance rate for DILI patients between the two algorithms was 79.4%; the Spearman rank correlation coefficient was 0.952 ($P < 0.0001$). Although the CIOMS/RUCAM scale does not explicitly define slowly metabolized chemicals, AM has a longer half-life than other drugs.

DOI: 10.1002/pds

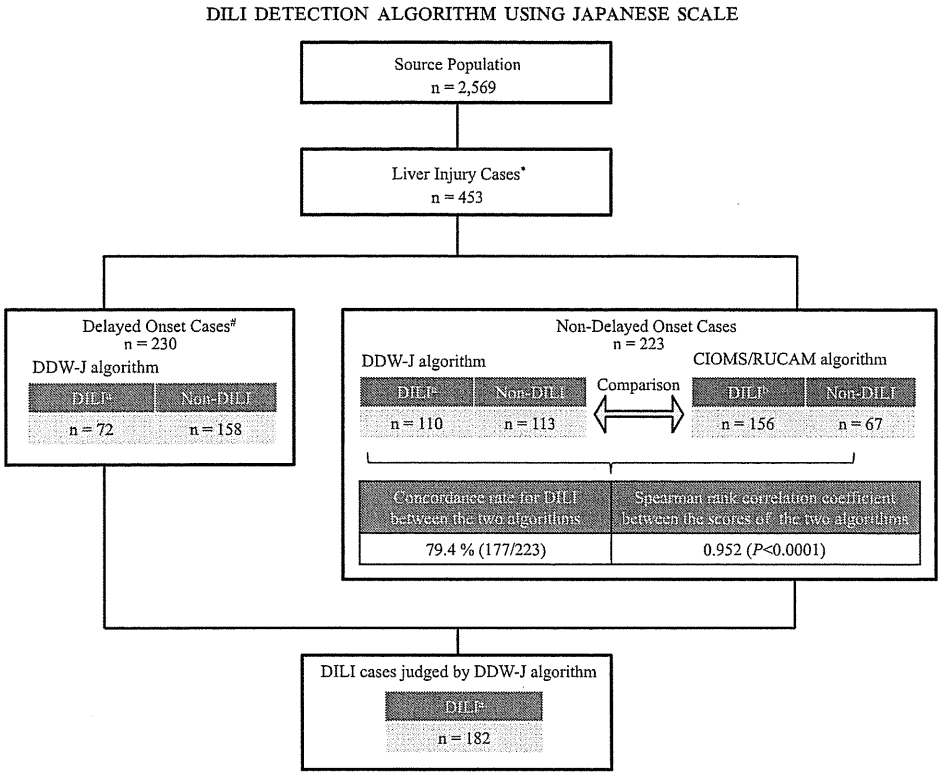

Figure 1. Identification of drug-induced liver injury (DILI) cases in the Hamamatsu population. *Patients with alanine aminotransferase > 2 × the upper limit of normal value (ULN) or alkaline phosphatase >ULN from the index date to 180 days after the last administration. #Patients in which the liver injury occurred after 15 days for the hepatocellular type, or more than 30 days for the cholestatic or mixed type, following the last administration. [a]Defined as a total score ≥5 in the Digestive Disease Week Japan 2004 (DDW-J) algorithm. [b]Defined as a total score ≥6 in the Council for International Organizations of Medical Sciences/the Roussel Uclaf Causality Assessment Method (CIOMS/RUCAM) algorithm

We therefore performed sensitivity analysis that incorporated the delayed onset cases prescribed AM into the comparison. This analysis showed consistent findings with a concordance rate of 78.4%.

Presence of possible alternative causes in DILI cases was compared with liver injury cases judged as non-DILI by the DDW-J algorithm in the Hamamatsu population (Table S2). The results showed that patients with alternative causes, such as viral hepatitis, were effectively excluded by this algorithm.

Characteristics of drug-induced liver injury patients

The study population sizes in MIDs from Hamamatsu and MDV were 2569 and 3856, respectively. To examine the characteristic of DILI patients, the ORs for DILI identified by the DDW-J algorithm were calculated (Table 1, with details in Table S3). The ORs of DILI onset in men were 1.44 (95% confidence interval, 1.05–1.98) in the Hamamatsu MID and 1.32 (95% confidence interval, 1.01–1.72) in the MDV MID. Because there were considerable differences in the average treatment duration, we performed an additional sub-analysis on treatment duration stratified by the study drugs. In the MDV MID, CM and LV subpopulations showed a significant association between a long treatment duration and DILI.

DISCUSSION

We demonstrated that the DDW-J algorithm was highly compatible with the CIOMS/RUCAM algorithm in the Hamamatsu MID (Figure 1). This indicates the DDW-J algorithm has adequate generalizability in assessing DILI. Using the DDW-J algorithm, we examined the characteristics of DILI cases by assessing the potential risk factors. Furthermore, we used the same study protocol to investigate a second population that included patients from multiple hospitals (MDV MID) to improve the robustness of our results. As a result, men showed a significantly higher risk for DILI in both populations. This finding is inconsistent with those of previous reports, although the role of gender in DILI remains controversial.[4] Alcohol consumption is one of the criteria in both the DDW-J and CIOMS/RUCAM scales, but this information was not available in the

DOI: 10.1002/pds

Table 1. Comparison of odds ratios (ORs) for onset of drug-induced liver injury (DILI) in two medical information databases (MIDs)

	Hamamatsu University Hospital MID				MDV MID			
Characteristics	*n*	OR*	95% CI	*P*-value	*n*	OR*	95% CI	*P*-value
Total	2569				3856			
Age ≥55 years		1.49	1.02–2.17	0.0371		0.85	0.63–1.16	0.3052
Male		1.44	1.05–1.98	0.0237		1.32	1.01–1.72	0.0409
Inpatient		1.38	1.01–1.90	0.0452		1.30	0.99–1.72	0.0624
Diabetes mellitus		0.81	0.47–1.38	0.4316		0.90	0.60–1.36	0.6225
Long treatment[a]		1.14	0.83–1.57	0.4225		1.46	1.10–1.94	0.0082
High dose[b]		1.83	0.81–4.16	0.1473		1.34	0.73–2.48	0.3436
Clarithromycin sub-group	524				845			
Days ≥8		1.19	0.56–2.52	0.6531		3.18	1.59–6.37	0.0011
Days ≥28		2.08	0.91–4.80	0.0846		2.97	1.43–6.15	0.0034
Levofloxacin sub-group	1551				2441			
Days ≥8		1.15	0.75–1.76	0.5273		1.57	1.10–2.23	0.0122

CI, confidence interval; DILI, defined as Digestive Disease Week Japan 2004 score ≥5.
[a]Patients whose treatment duration was ≥8 days in clarithromycin, levofloxacin, and moxifloxacin and ≥4 days in azithromycin.
[b]Patients whose average dose was beyond the usual approved dose.
*Adjusted for age (≥55 years), gender, in/outpatient status, diabetes mellitus, treatment duration, and high dose.

current study. Because the national survey in Japan indicated that alcohol consumption was remarkably higher in men than in women (35.1% vs. 7.7%),[13] the gender difference in alcohol consumption might have led to a higher risk in men.

Regarding treatment duration, a longer treatment with CM and LX, which included an adequate population size in this study, was significantly associated with DILI in the MDV population. In the Hamamatsu population, the long treatment groups, especially the ≥28-day CM group, showed a tendency toward a higher risk for DILI, although the associations were not significant. These results might indicate that DILI should be carefully monitored during the long-term treatments with antibiotics. Although further confirmation in a larger-scale study is necessary, our algorithm, which is based on a clinical diagnostic scale, could be a useful method to identify DILI and access its risk-related information through MID research.

The current study has some limitations. The DDW-J and CIOMS/RUCAM scoring systems were designed for prospective diagnoses of individual cases, and their utilities in retrospective studies, including the quality of DILI cases identified by our algorithms, were not validated. Furthermore, we could not retrieve additional information from the MIDs used in this study, such as drinking habits and pregnancy, which constitutes parts of the scoring systems. This might lead to underestimation of DILI risk. In addition, articles on the DDW-J were predominantly published in Japanese-language journals, which makes it difficult for non-Japanese researchers to assess and utilize the DDW-J scale. Although regional DILI scoring would still be required for diagnostic purpose when considering the Japanese medical environment, the adoption of a uniform diagnostic approach will be preferable in future.

In conclusion, we have proposed a useful method that uses MIDs for identifying DILI. Our study supports the utility of MID research in pharmacovigilance.

CONFLICT OF INTEREST

The authors declare no conflict of interest.

KEY POINTS
- A standardized detection method for DILI using MIDs has not yet been established because of the complexity of diagnosis.
- We applied a Japanese DILI diagnostic scale, DDW-J, to a DILI detection algorithm that is applicable for assessment of potential risk factors.
- The DDW-J algorithm was compatible with the international CIOMS/RUCAM scale, which indicates the utility of the algorithm.
- This study supports the utility of MID-based research for improving pharmacovigilance.

ETHICS STATEMENT

This study was approved, including procedures for informed consent, by the ethics committees of both the Hamamatsu University School of Medicine and the National Institute of Health Sciences.

DOI: 10.1002/pds

ACKNOWLEDGEMENTS

We thank Ms. Kaori Ota and Mr. Masaki Nakamura (MDV) for their technical support. This study was supported by the Program for the Promotion of Studies in Health Science from the Ministry of Health, Labour and Welfare of Japan (H23-iyaku-shitei-025). The authors' research was conducted independently of the funding organization.

REFERENCES

1. Aithal GP, Watkins PB, Andrade RJ, *et al.* Case definition and phenotype standardization in drug-induced liver injury. *Clin Pharmacol Ther* 2011; **89**: 806–815.
2. Sgro C, Clinard F, Ouazir K, *et al.* Incidence of drug-induced hepatic injuries: a French population-based study. *Hepatology* 2002; **36**: 451–455.
3. Navarro VJ, Senior JR. Drug-related hepatotoxicity. *N Engl J Med* 2006; **354**: 731–739.
4. Chalasani N, Björnsson E. Risk factors for idiosyncratic drug-induced liver injury. *Gastroenterology* 2010; **138**: 2246–2259.
5. Lucena MI, García-Cortés M, Cueto R, *et al.* Assessment of drug-induced liver injury in clinical practice. *Fundam Clin Pharmacol* 2008; **22**: 141–158.
6. Danan G, Benichou C. Causality assessment of adverse reactions to drugs-I. A novel method based on the conclusions of international consensus meetings: application to drug-induced liver injuries. *J Clin Epidemiol* 1993; **46**: 1323–1330.
7. Tajiri K, Shimizu Y. Practical guidelines for diagnosis and early management of drug-induced liver injury. *World J Gastroenterol* 2008; **14**: 6774–6785.
8. Watanabe M, Shibuya A, Miura Y, *et al.* Validity study of DDW-J2004 scoring scale for drug-induced liver injury. *Kanzo* 2007; **48**: 219–226. [In Japanese]
9. Shin J, Hunt CM, Suzuki A, *et al.* Characterizing phenotypes and outcomes of drug-associated liver injury using electronic medical record data. *Pharmacoepidemiol Drug Saf* 2013; **22**: 190–198.
10. Lo Re V, 3rd, Haynes K, Goldberg D, *et al.* Validity of diagnostic codes to identify cases of severe acute liver injury in the US Food and Drug Administration's Mini-Sentinel Distributed Database. *Pharmacoepidemiol Drug Saf* 2013; **22**: 861–872.
11. Kimura M, Tani S, Watanabe H, *et al.* High speed clinical data retrieval system with event time sequence feature: with 10 years of clinical data of Hamamatsu University Hospital CPOE. *Methods Inf Med* 2008; **47**: 560–568.
12. Takikawa H, Onji M, Takamori Y, *et al.* Proposal of diagnostic criteria for drug-induced liver injury revised by the DDW-J 2004 workshop. *Kanzo* 2005; **46**: 85–90. [In Japanese]
13. Ministry of Health, Labour and Welfare. National Health and Nutrition Survey in 2011. Ministry of Health, Labour and Welfare, Tokyo; March 2013. http://www.mhlw.go.jp/bunya/kenkou/eiyou/dl/h23-houkoku.pdf [9 January 2014]. [In Japanese]

SUPPORTING INFORMATION

Additional supporting information may be found in the online version of this article at the publisher's web site.

Biochemical Pharmacology 86 (2013) 428–436

Contents lists available at SciVerse ScienceDirect

Biochemical Pharmacology

journal homepage: www.elsevier.com/locate/biochempharm

Dual roles of nuclear receptor liver X receptor α (LXRα) in the *CYP3A4* expression in human hepatocytes as a positive and negative regulator

Keisuke Watanabe, Kaori Sakurai, Yuri Tsuchiya, Yasushi Yamazoe, Kouichi Yoshinari *

Division of Drug Metabolism and Molecular Toxicology, Graduate School of Pharmaceutical Sciences, Tohoku University, Japan

ARTICLE INFO

Article history:
Received 9 April 2013
Accepted 22 May 2013
Available online 31 May 2013

Keywords:
Enzyme induction
Nuclear receptor
Cholesterol homeostasis
Human hepatocyte
Transcriptional crosstalk

ABSTRACT

CYP3A4 is a major drug-metabolizing enzyme in humans, whose expression levels show large inter-individual variations and are associated with several factors such as genetic polymorphism, physiological and disease status, diet and xenobiotic exposure. Nuclear receptor pregnane X receptor (PXR) is a key transcription factor for the xenobiotic-mediated transcription of *CYP3A4*. In this study, we have investigated a possible involvement of liver X receptor α (LXRα), a critical regulator of cholesterol homeostasis, in the hepatic *CYP3A4* expression since several recent reports suggest the involvement of CYP3A enzymes in the cholesterol metabolism in humans and mice. Reporter assays using wild-type and mutated *CYP3A4* luciferase reporter plasmids and electrophoretic mobility shift assays revealed that LXRα up-regulated *CYP3A4* through the known DNA elements critical for the PXR-dependent *CYP3A4* transcription, suggesting LXRα as a positive regulator for the *CYP3A4* expression and a crosstalk between PXR and LXRα in the expression. In fact, reporter assays showed that LXRα activation attenuated the PXR-dependent *CYP3A4* transcription. Moreover, a PXR agonist treatment-dependent increase in *CYP3A4* mRNA levels was suppressed by co-treatment with an LXRα agonist in human primary hepatocytes and HepaRG cells. The suppression was not observed when LXRα expression was knocked-down in HepaRG cells. In conclusion, the present results suggest that sterol-sensitive LXRα positively regulates the basal expression of *CYP3A4* but suppresses the xenobiotic/PXR-dependent *CYP3A4* expression in human hepatocytes. Therefore, nutritional, physiological and disease conditions affecting LXRα might be one of the determinants for the basal and xenobiotic-responsive expression of *CYP3A4* in human livers.

1. Introduction

CYP3A4 is a major drug-metabolizing enzyme in human. It is highly expressed in the liver and small intestine, and contributes to the disposition of about half of clinically used pharmaceutical drugs [1–4]. The expression levels of hepatic CYP3A4 show large inter-individual variations, which results in the inter-individual variations of pharmacokinetics, efficacy and adverse side effects of therapeutic drugs. The precise reason for the variation remains unknown, but several factors such as genetic polymorphism, age, sex, physiological status, disease, diet, and xenobiotic exposure are known to be involved [5,6].

The molecular mechanism for the xenobiotic-induced expression of *CYP3A4* (CYP3A4 induction) has been increasingly understood. Xenobiotic-responsive nuclear receptors pregnane X receptor (PXR; NR1I2) and constitutive active/androstane receptor (CAR; NR1I3) play central roles in this CYP3A4 induction. These nuclear receptors were reported to bind to two cis-elements termed dNR1 and prER6 found in the *CYP3A4* distal and proximal promoter, respectively [7–10], as a heterodimer with retinoid X receptor (RXR) to enhance the transcription of *CYP3A4*. Recently, we have identified another PXR-responsive element, termed eNR3A4, located very close to dNR1 [11]. This motif comprises the direct repeat separated by 4 nucleotides (DR-4). Interestingly, the lack of functional eNR3A4 completely removed the responsiveness of reporter genes to the ligand-activated PXR in cell-based reporter assays using HepG2 cells and human hepatocytes, despite that the reporter genes contained both dNR1 and prER6 motifs [11]. These results suggest the critical role of eNR3A4 in the PXR-mediated expression of *CYP3A4* in hepatocytes.

Abbreviations: 24S-HC, 24(S)-hydroxycholesterol; CAR, constitutive active/androstane receptor; CITCO, 6-(4-chlorophenyl)imidazo[2,1-b][1,3]thiazole-5-carbaldehyde-O-(3,4-dichlorobenzyl)oxime; DMSO, dimethyl sulfoxide; DR-4, direct repeat separated by 4 nucleotides; EMSA, electrophoretic mobility shift assays; ER-6, everted repeat separated by 6 nucleotides; LXRα, liver X receptor α; PXR, pregnane X receptor; qRT-PCR, quantitative reverse transcription-PCR; RXR, retinoid X receptor; SREBP-2, sterol regulatory element-binding protein-2.

* Corresponding author.
E-mail address: yoshinari@m.tohoku.ac.jp (K. Yoshinari).

0006-2952/$ – see front matter © 2013 Elsevier Inc. All rights reserved.
http://dx.doi.org/10.1016/j.bcp.2013.05.016

In addition to its central role in the drug metabolism, CYP3A4 is known to also mediate sterol oxidation. Bodin et al. [12] demonstrated that recombinant CYP3A4, but not CYP1A2, CYP2B6 and CYP2C9, catalyzed 4β-hydroxylation of cholesterol in vitro and that plasma 4β-hydroxycholesterol levels were higher in patients treated with antiepileptic drugs known as CYP3A4 inducers, such as carbamazepine, phenytoin and phenobarbital, than in healthy volunteers. Treatment with other CYP3A4 inducers rifampicin and efavirenz also increased plasma 4β-hydroxycholesterol concentrations in healthy subjects and HIV-1-infected patients, respectively [13,14]. The involvement of CYP3A4 in the metabolism of bile acids, which are synthesized from cholesterol, is also demonstrated. CYP3A4 mediated 6β-hydroxylation of taurochenodeoxycholic acid and lithocholic acid [15], 1β-hydroxylation of deoxycholic acid [16], and the formation of 3-dehydrocholic acid and γ-muricholic acid from cholic acid and chenodeoxycholic acid, respectively [17]. The association of CYP3A enzymes with cholesterol and bile acid metabolism has also been reported in mice [18,19]. Interestingly, we have recently reported in mice that hepatic *Cyp3a11* expression is down-regulated by reduced intake of dietary cholesterol through a mechanism involving sterol regulatory element-binding protein-2 (SREBP-2) [20]. These results suggest a possible role of hepatic CYP3A enzymes in cholesterol homeostasis.

Liver X receptor α (LXRα), a member of the nuclear receptor superfamily, plays critical roles in cholesterol homeostasis [21]. The receptor is activated by oxysterols including 4β-hydroxycholesterol and 24(*S*)-hydroxycholesterol (24S-HC), and transactivates numbers of genes associated with cholesterol metabolism and transport including those encoding CYP7A1, SREBP-1c, lipoprotein lipase, cholesterol ester transfer protein, ABCA1, ABCG5 and ABCG8 [21–23]. LXRα exhibits some similarities with PXR and CAR, being highly expressed in the liver and preferring DR-4 type motifs as its binding motifs [24].

These facts mentioned above have raised the possibility that LXRα is involved in the gene regulation of *CYP3A4*. In the present study, we have investigated this possibility. We here show that LXRα is a positive regulator for the constitutive expression of *CYP3A4* but acts as a suppressor of the PXR-mediated expression of *CYP3A4* in human hepatocytes, indicating a unique role of LXRα in the hepatic *CYP3A4* expression.

2. Materials and methods

2.1. Materials

T4 polynucleotide kinase and restriction enzymes were purchased from New England Biolabs (Ipswich, MA). Poly(dI-dC) and [γ-^{32}P] ATP were purchased from GE Healthcare (Piscataway, NJ) and PerkinElmer (Waltham, MA), respectively. Rifampicin and 24S-HC were purchased from Sigma–Aldrich (St. Louis, MO). T0901317 and 6-(4-chlorophenyl)imidazo[2,1-b][1,3]thiazole-5-carbaldehyde-O-(3,4-dichlorobenzyl)oxime (CITCO) were purchased from Cayman Chemical (Ann Arbor, MI) and MERCK (Darmstadt, Germany), respectively. All other chemicals were from Wako Pure Chemicals (Osaka, Japan) or Sigma–Aldrich, unless otherwise mentioned. Oligonucleotides were commercially synthesized by Fasmac (Atsugi, Japan).

2.2. Plasmid DNA

hLXRα mammalian expression plasmid (pTarget-hLXRα) with pTarget (Promega, Madison, WI) and its pTNT (Promega)-based plasmid for in vitro synthesis were prepared in our laboratory [25]. pTarget-hRXRα, pTNT-hPXR, and pTNT-hRXRα were reported previously [11,26].

p3A4, previously called pCYP3A4-362-7.7k, and its deleted and mutated constructs other than p3A4-m4 and p3A4-m5 were prepared previously [11].

p3A4-m4 and p3A4-m5 were prepared by using KOD-Plus-Mutagenesis Kit (TOYOBO) as follows: PCR was carried out using the primers, 5′-CTCGAGCAGGTGAATCACAAGCTGAACTTCT-3′ and 5′-ACACAGGACAAGGTTTAATAATCACTG-3′, with p3A4-m3 for p3A4-m4 or p3A4-m1 for p3A4-m5 as a template. The PCR products were digested with DpnI and self-ligated by Ligation High and T4 Polynucleotide kinase.

(dNR1)$_5$-pGL3 and (eNR3A4)$_5$-pGL3 were prepared as follows: oligonucleotides for (dNR1)$_5$-pGL3, 5′-GTACC(GAATGAACTTGCT-GACCCTCT)$_5$G-3′ and 5′-CTAGC(AGAGGGTCAGCAAGTTGATTC)$_5$G-3′, and those for (eNR3A4)$_5$-pGL3, 5′-CTAGC(CCTTGTCCTGTGTT-GACCCCAG)$_5$A-3′ and 5′-GATCT(CTGGGGTCAACACAGGA-CAAGG)$_5$G-3, were annealed and ligated into the Acc65I/NheI or NheI/BglII sites of pGL3 promoter vector (Promega) using Ligation High (TOYOBO).

2.3. Cell culture and reporter assays

HepG2 cells (RIKEN BioResource Center, Tsukuba, Japan) were cultured in Dulbecco's modified Eagle's medium supplemented with 10% heat-inactivated fetal bovine serum (Nichirei Biosciences, Tokyo, Japan), minimum essential medium nonessential amino acids, and Antibiotic-Antimycotic (Life Technologies, Carlsbad, CA). The cells were seeded in 48-well plates (BD Biosciences, Heidelberg, Germany) at 3×10^4 cells/well 24 h before transfection. Reporter construct and pTarget expression plasmid were cotransfected using calcium phosphate method. phRL-TK Control Vector (Promega) was also cotransfected to normalize transfection efficiency. Twelve hours after transfection, the cells were treated with chemicals as indicated in figure legends for 24 or 48 h in Dulbecco's modified Eagle's medium without fetal bovine serum. Thereafter, the cells were harvested, and firefly luciferase and *Renilla* luciferase activities were determined as described previously [26].

2.4. Electrophoretic mobility shift assays (EMSAs)

EMSAs were performed as described previously [11]. hPXR, hLXRα and hRXRα were synthesized in vitro with the corresponding pTNT plasmid, using TNT SP6 Quick-Coupled Transcription/Translation System (Promega). Control lysate was prepared using empty pTNT. The probe sequences used are shown in the legend to Fig. 2D.

2.5. Human hepatocyte culture

Cryopreserved human hepatocytes (lot. HEP187111; white, female, 56-year old, HEP187190; white, female, 72-year old, Hu4201; white, female, 63-year old), purchased from Biopredic International (Rennes, France) or Life Technologies, were thawed using Hepatocytes Isolation Kit (Xenotech, Lenexa, KS) according to the manufacture's protocol. The cells were plated onto collagen-coated 48-well plates (BD Biosciences) at a density of 2×10^5 cells/well and maintained in KHEM5310 medium (KAC, Kyoto, Japan) supplemented with 10% fetal bovine serum for 4 h in an atmosphere of 5% CO_2/95% air at 37 °C. The medium was then changed to serum-free Williams' medium E (Life Technologies) containing 0.1 μM dexamethasone (Sigma–Aldrich), ITS-PREMIX (BD Bioscience), 100 U/ml penicillin (Life Technologies) and 100 μg/ml streptomycin (Life Technologies), and the cells were cultured for 24 h. The medium was changed to that containing various chemicals, and the cells were cultured for additional 48 h with medium renewal after 24 h.

Table 1
Primers used for qRT-PCR.

Gene	Forward (5′–3′)	Reverse (5′–3′)
CYP3A4	CACAGATCCCCCTGAAATTAAGCTTA	AAAATTCAGGCTCCACTTACGGTG
CYP2B6	CATCATCCCCAAGGACACAG	AAATCCGCTTCCCTAAGGAG
ABCA1	GGCCTTGGCCTTTGTCGGGG	TGGTGCGGCCTTGTCGGTAT
LXRα	TCTCCCAGCAAGGGGGCTCC	AGCTCCACCGCAGAGTCAGGA
ACTB	GCCAACACAGTGCTGTCTG	CCTGCTTGCTGATCCACATC

2.6. HepaRG cell culture

Differentiated HepaRG cells (lot, HepaRG933777 and HepaRG1224919) purchased from Life Technologies were thawed using Working medium (Life Technologies) according to the manufacture's protocol. The cells were plated onto collagen-coated 48-well plates at a density of 2×10^5 cells/well and cultured in an atmosphere of 5% CO_2/95% air at 37 °C. Six hours later, the medium was changed to the fresh Working medium and the cells were cultured for additional 66 h. The cells were then cultured in Induction medium (Life Technologies) containing vehicle (0.2% dimethyl sulfoxide (DMSO), Wako Pure Chemicals) or various drugs for 48 h with medium renewal after 24 h.

2.7. Quantitative reverse transcription-PCR (qRT-PCR)

Total RNA was prepared from human hepatocytes and HepaRG cells using SV total RNA Isolation System (Promega) according to the manufacture's protocol. cDNA was synthesized using High-Capacity cDNA Reverse Transcription Kit (Applied Biosystems), and quantitative PCR was performed with ABI7000 (Applied Biosystems) using GoTaq qPCR Master Mix (Promega) and primers shown in Table 1.

2.8. siRNA transfection

HepaRG cells were thawed and cultured as mentioned above except that 24-well plates were used. After 72 h from seeding, human LXRα (hLXRα)-targeting siRNAs (Life Technologies) were transfected using INTERFERin (Polyplus transfection) according to the manufacture's protocol. Forty-eight hours after transfection, the cells were cultured in Induction medium (Life Technologies) containing vehicle (0.2% DMSO) or various drugs for 48 h. In this study, 2 different hLXRα-targeting siRNAs were used. Their sequences were 5′-UUCCACAUAUGUGUGCUGCAGCCUC-3′ and 5′-AGAAGCAUCACCUCGAUCGCAGAGG-3′. Slicer negative control siRNA (Applied Biosystems) was used as a control siRNA.

2.9. Statistical analysis

Prism version 4.0 (GraphPad Software, San Diego, CA) was used for all the statistical analyses.

3. Results

3.1. hLXRα-mediated transcription of CYP3A4

To investigate whether LXRα is involved in the gene regulation of *CYP3A4*, we first performed reporter assays using *CYP3A4* luciferase reporter plasmid (p3A4) in HepG2 cells (Fig. 1). Co-transfection of hLXRα-expressing plasmid and treatment with LXRα agonists, GW3965 or 24S-HC, resulted in the significant increase in reporter activities about 3–10-fold. These results suggest that ligand-activated hLXRα is able to transactivate *CYP3A4*.

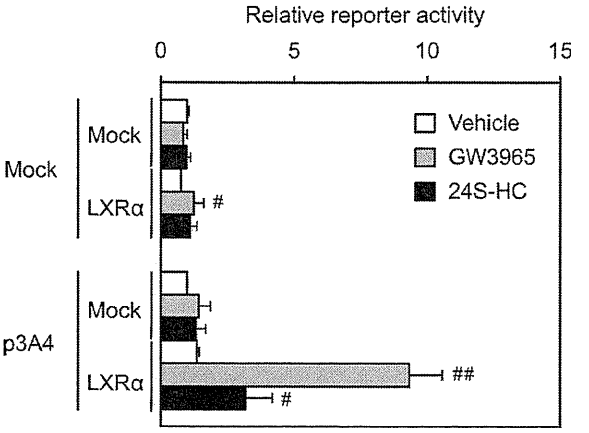

Fig. 1. hLXRα-mediated transactivation of *CYP3A4*. HepG2 cells (3×10^4 cells/well in 48-well plate) were transfected with each reporter plasmid (0.5 μg), phRL-TK (0.025 μg) and either pTarget-hLXRα or empty pTarget (0.1 μg). Twenty hours after transfection, the cells were treated with vehicle (0.1% DMSO), GW3965 (2 μM) or 24S-HC (10 μM) for 48 h, and reporter activities were measured. Firefly luciferase activities were normalized with *Renilla* luciferase activities. Data are expressed as relative activities to those in vehicle-treated cells for each reporter construct. Data are the mean ± SD ($n = 4$) of one representative experiment from 2 independent experiments. $^{\#}P < 0.05$; $^{\#\#}P < 0.01$, significantly different from the corresponding vehicle-treated cells based on one-way ANOVA followed by Dunnett's post hoc test.

3.2. Identification of hLXRα-responsive elements in the CYP3A4 promoter

To identify an hLXRα-responsive region, we performed reporter assays using various deletion constructs (Fig. 2A). When the region from −7836 to −7494 was deleted, reporter activity was hardly increased in response to the hLXRα activation. When the region from −7607 to −7216 was deleted, the hLXRα-responsiveness was greatly but not completely removed. However, when the region from −7836 to −7737 or that from −7494 to −7200 was deleted, the hLXRα-responsiveness was not altered. These results suggest that two regions, one from −7738 to −7608 and the other from −7607 to −7216, are essential for the hLXRα-dependent transactivation of *CYP3A4*.

Previous studies identified two hPXR responsive elements, termed dNR1 and prER6, in the distal and proximal *CYP3A4* promoter, respectively [7–10]. In addition, we have recently identified another hPXR-responsive element, termed eNR3A4, close to dNR1 [11]. dNR1, eNR3A4 and prER6 are DR-3 (direct repeat separated by 3 nucleotides)-, ER-6 (everted repeat separated by 6 nucleotides)- and DR-4-type motifs, respectively. Since LXRα preferentially binds to DR4-type motifs as does PXR, we examined whether these hPXR-responsive elements could work for the hLXRα-mediated *CYP3A4* transcription, using reporter assays with mutated p3A4 constructs (Fig. 2B). The hLXRα-responsiveness of the prER6-mutated construct (p3A4-m1) was as high as that of the wild-type construct. However, the introduction of a mutation into eNR3A4 or dNR1 decreased *CYP3A4* transactivation in response to the hLXRα activation (p3A4-m2 and p3A4-m3). Moreover, mutating both dNR1 and eNR3A4 simultaneously abolished the hLXRα-responsiveness completely (p3A4-m4). Besides, mutating both eNR3A4 and prER6 greatly but not completely decreased *CYP3A4* transactivation in response to the hLXRα activation (p3A4-m5), while mutating both dNR1 and prER6 completely abolished the hLXRα-responsiveness (p3A4-m6). These results suggest that the transcription of *CYP3A4* by hLXRα is mainly mediated through dNR1 and eNR3A4.

Next, to confirm the role of dNR1 and eNR3A4 in the transcription of *CYP3A4* by hLXRα, we prepared two reporter

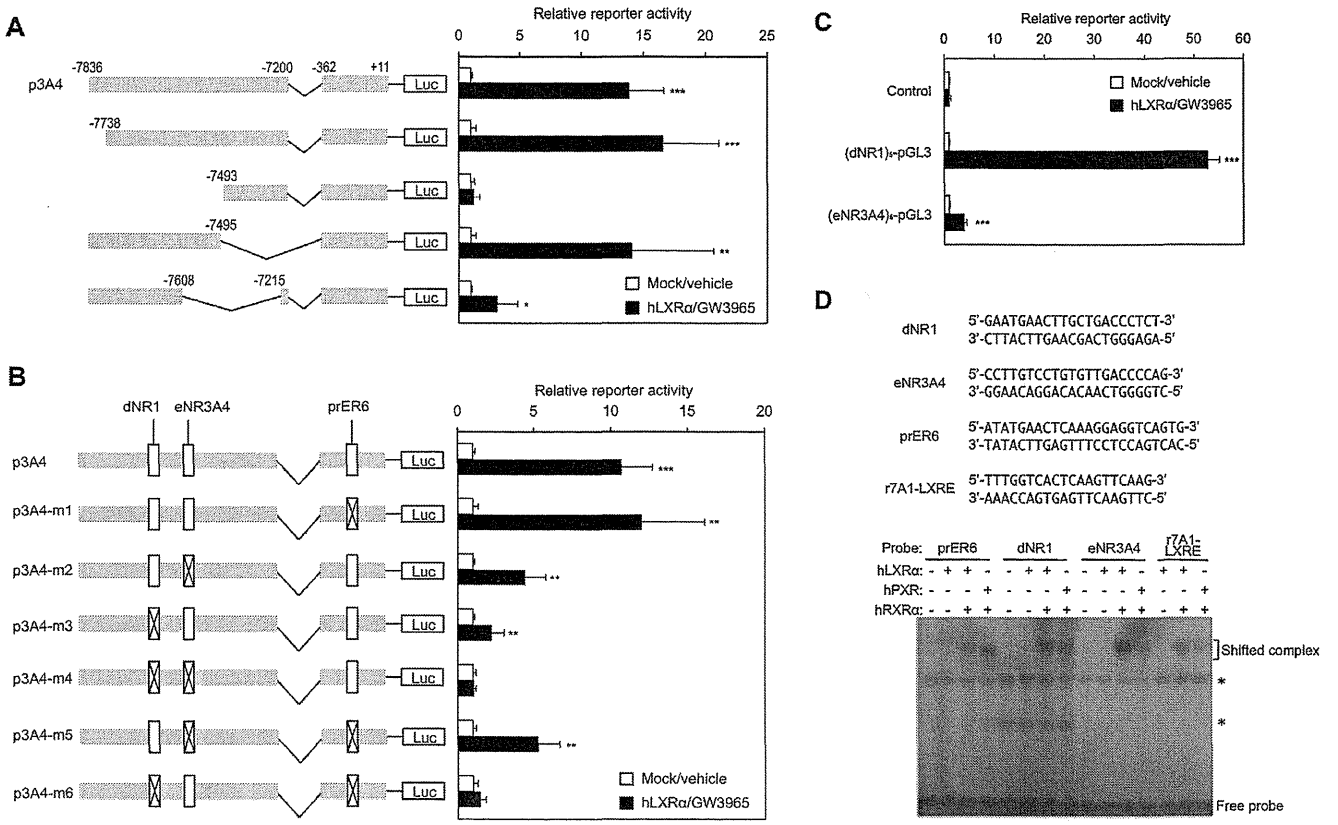

Fig. 2. Identification of the hLXRα-responsive elements in the *CYP3A4* promoter. (A) and (B) HepG2 cells were seeded and transfected with plasmid DNA as in Fig. 1. Twelve hours after transfection, the cells were treated with vehicle (0.1% DMSO) or GW3965 (2 μM) for 48 h and harvested, and reporter activities were determined as described in Section 2. The numbers above the constructs indicate the positions relative to the transcription start site. Firefly luciferase activities normalized with *Renilla* luciferase activities are shown as ratio to those in control cells (Mock/vehicle) for each reporter construct. Data are the mean ± SD ($n = 4$) of one representative experiment from 2 independent experiments. (C) HepG2 cells seeded in 48-well plates at density of 3×10^4 cells/well were transfected with 0.2 μg of reporter construct (pGL3-promoter (Control), $(dNR1)_5$-pGL3 or $(eNR3A4)_5$-pGL3), 0.05 μg of expression plasmid, and 0.0125 μg of phRL-TK. The cells were treated with vehicle (0.1% DMSO) or GW3965 (2 μM) for 24 h, and reporter activities were determined. The results are presented as in (A) and (B). Data are the mean ± SD ($n = 4$) of one representative experiment from 2 independent experiments. (D) EMSAs were performed as described in Section 2 with radiolabeled oligonucleotides shown above and in vitro synthesized nuclear receptors. Asterisks represent non-specific bindings. Student's *t*-test was performed between two groups indicated; $^*P < 0.05$; $^{**}P < 0.01$; $^{***}P < 0.001$.

constructs, which contain five copies of dNR1 or eNR3A4, termed $(dNR1)_5$-pGL3 or $(eNR3A4)_5$-pGL3, respectively, and carried out reporter assays using these constructs. As shown in Fig. 2C, hLXRα transactivated these reporter constructs with a preference for $(dNR1)_5$-pGL3. These results further corroborate the idea that the transcription of *CYP3A4* by hLXRα is mediated through dNR1 and eNR3A4.

Finally, we carried out EMSAs to investigate the binding of hLXRα to dNR1, eNR3A4 and prER6. The probe containing the rat *Cyp7a1* LXR-responsive element (r7A1-LXRE) was used as a positive control for the hLXRα/hRXRα binding. As shown in Fig. 2D, the hLXRα/hRXRα heterodimer bound to prER6, dNR1 and eNR3A4 as well as the positive control probe, but hLXRα alone did not bind to either probe.

3.3. Influences of hLXRα activation on the hPXR-dependent CYP3A4 transcription in reporter assays

The results shown above suggest that hLXRα transactivates *CYP3A4* through the hPXR-responsive elements, raising a possibility of the crosstalk between these nuclear receptors for the *CYP3A4* transcription. To test this possibility, we investigated the influences of individual and simultaneous activations of hLXRα and hPXR on the *CYP3A4* expression in reporter assays (Fig. 3A). Reporter activities were increased 7-fold and 19-fold by either hLXRα or hPXR activation, respectively. Interestingly, when both receptors were expressed, reporter activities after simultaneous treatment with their agonists were intermediate between those after single treatment with rifampicin or GW3965. Under this condition, the expression levels of PXR, assessed by Western blotting, were not decreased by co-expression of LXRα (data not shown). These results suggest that hLXRα has a weaker ability to activate *CYP3A4* transcription than hPXR and might compete with hPXR for the transcription. To investigate this possibility, we carried out similar experiments using the hPXR/hLXRα dual-agonist, T0901317 (Fig. 3B). The T0901317 treatment-dependent increase in reporter activities was much greater when hPXR was expressed alone than when hLXRα was expressed alone, which is consistent with the results obtained in Fig. 3A using individual ligands. As expected, the T0901317-dependent increase in the reporter activity in cells where both receptors were co-expressed was intermediate between those in cells where either hLXRα or hPXR was expressed alone.

Both PXR and LXRα form a heterodimer with RXRα to transactivate their target genes. We thus investigated whether the amount of RXRα was a limiting factor for the *CYP3A4* transcription by simultaneous activation of hPXR and hLXRα (Fig. 3C). hRXRα overexpression enhanced the hPXR-mediated and hLXRα-mediated expression of *CYP3A4*. Even under these conditions, hPXR-mediated *CYP3A4* expression was suppressed by co-activation of hLXRα (compare closed and hatched bars with 100 ng or 300 ng of hRXRα plasmid).

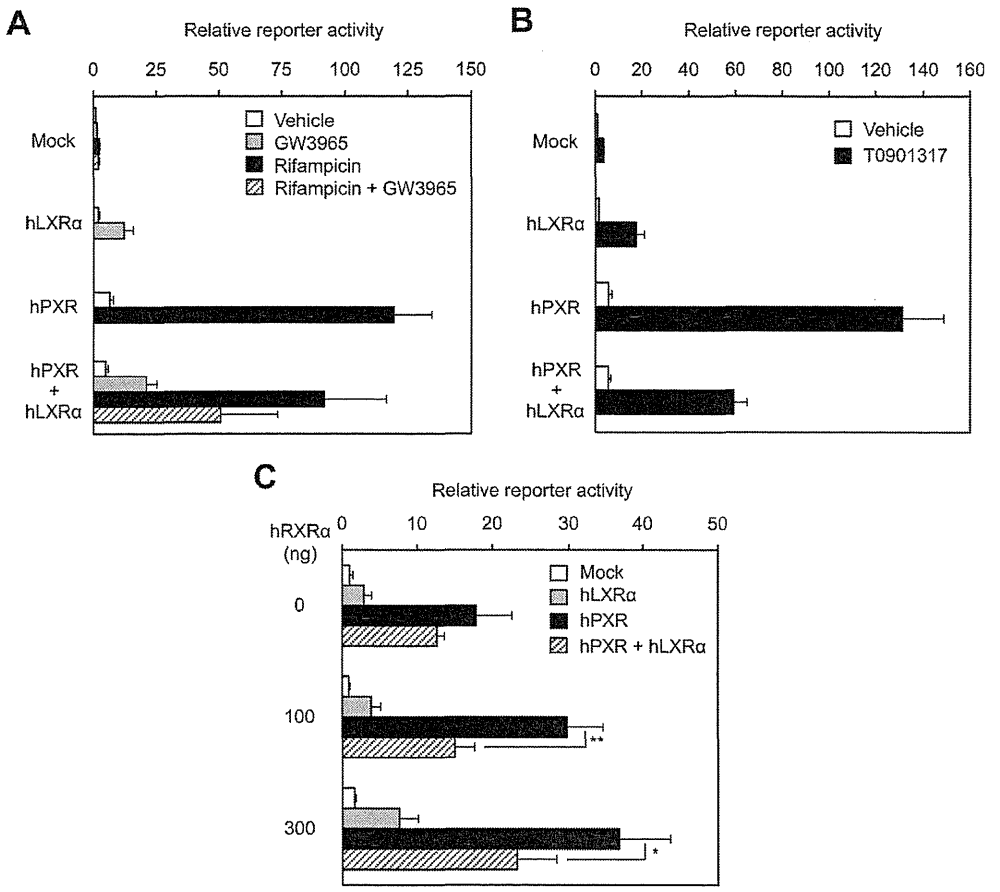

Fig. 3. Influences of hLXRα activation on the PXR-dependent *CYP3A4* transactivation in reporter assays. (A) and (B) HepG2 cells (3×10^4 cells/well in 48-well plate) were transfected with p3A4 (0.5 μg), phRL-TK (0.025 μg) and expression plasmids (hLXRα; pTarget-hLXRα (0.05 μg) and empty pTarget (0.05 μg), hPXR; pTarget-hPXR (0.05 μg) and empty pTarget (0.05 μg), hPXR + hLXRα; pTarget-hPXR (0.05 μg) and pTarget-hLXRα (0.05 μg)). Twenty hours after transfection, the cells were treated with vehicle (0.2% DMSO), T0901317 (1 μM), GW3965 (2 μM) or rifampicin (10 μM) for 48 h, and reporter activities were measured. Firefly luciferase activities were normalized with *Renilla* luciferase activities. (C) HepG2 cells were seeded and transfected with plasmid DNA as in (A) and (B) except that pTarget-hRXRα was also used. Twenty hours after transfection, the cells were treated with T0901317 (1 μM) for 48 h, and reporter activities were measured. Firefly luciferase activities were normalized with *Renilla* luciferase activities. Data are expressed as relative activities to those in mock-transfected and vehicle-treated cells (top bar in each figure). Data are the mean ± SD ($n = 4$) of one representative experiment from 3 independent experiments. Student's *t*-test was performed between two groups indicated; $^*P < 0.05$; $^{**}P < 0.01$.

3.4. Influences of GW3965 treatment on CYP3A4 mRNA levels in human hepatocytes

The results of reporter assays suggest that ligand-activated hLXRα enhances *CYP3A4* expression but suppresses the hPXR-induced transcription. We thus examined whether this could be observed in human hepatocytes. First, differentiated HepaRG cells, which show similar characteristics with human hepatocytes in terms of the expression of drug metabolizing enzymes, were treated with rifampicin in the absence or presence of GW3965, and *CYP3A4* mRNA levels were determined (Fig. 4A). As expected, *CYP3A4* mRNA levels were increased by treatment with GW3965 (3-fold). Moreover, rifampicin treatment was less effective in the presence of GW3065 (2-fold) than in the absence of GW3965 (11-fold), and the mRNA levels were significantly lower in the cells treated with both ligands than in the cells treated with rifampicin alone. We next performed similar experiments using three lots of primary human hepatocytes (Fig. 4B). Although treatment with GW3965 did not increase *CYP3A4* mRNA levels in these lots of hepatocytes, GW3965 co-treatment blocked the rifampicin-induced increase in the mRNA levels to various extents.

PXR regulates the expression of other CYP genes such as *CYP2B6* [27]. We thus investigated whether the hLXRα-mediated suppression was also observed in *CYP2B6* mRNA levels (Fig. 4C). The mRNA levels were increased by treatment with rifampicin or CITCO (a representative hCAR agonist). However, GW3965 co-treatment completely blocked the rifampicin- or CITCO-induced increase in the mRNA levels. Interestingly, treatment with GW3965 alone significantly reduced *CYP2B6* mRNA levels. *CYP2C8* mRNA levels were also increased by rifampicin treatment, and the increase was blocked by GW3965 co-treatment (data not shown).

3.5. Influence of hLXRα knockdown on GW3965- and/or rifampicin-induced changes in CYP3A4 mRNA levels

To further investigate the inhibitory effects of hLXRα on the hPXR-mediated *CYP3A4* expression, we transfected *hLXRα*-targeting siRNA into HepaRG cells, and mRNA levels of *CYP3A4* as well as *LXRα* and *ABCA1*, both of which are target genes of LXRα, were determined after rifampicin and/or GW3965 treatment (Fig. 5). GW3965 treatment increased mRNA levels of both *LXRα* and *ABCA1* in the mock-transfected cells. Knockdown of hLXRα significantly decreased *LXRα* mRNA levels both in vehicle- or GW3965-treated cells. *ABCA1* mRNA levels were also significantly decreased by hLXRα knockdown in the GW3965-treated cells. *CYP3A4* mRNA levels were significantly decreased by hLXRα knockdown (compare open bars in right panel). In the control siRNA-transfected cells, the rifampicin-dependent increase in *CYP3A4* mRNA levels

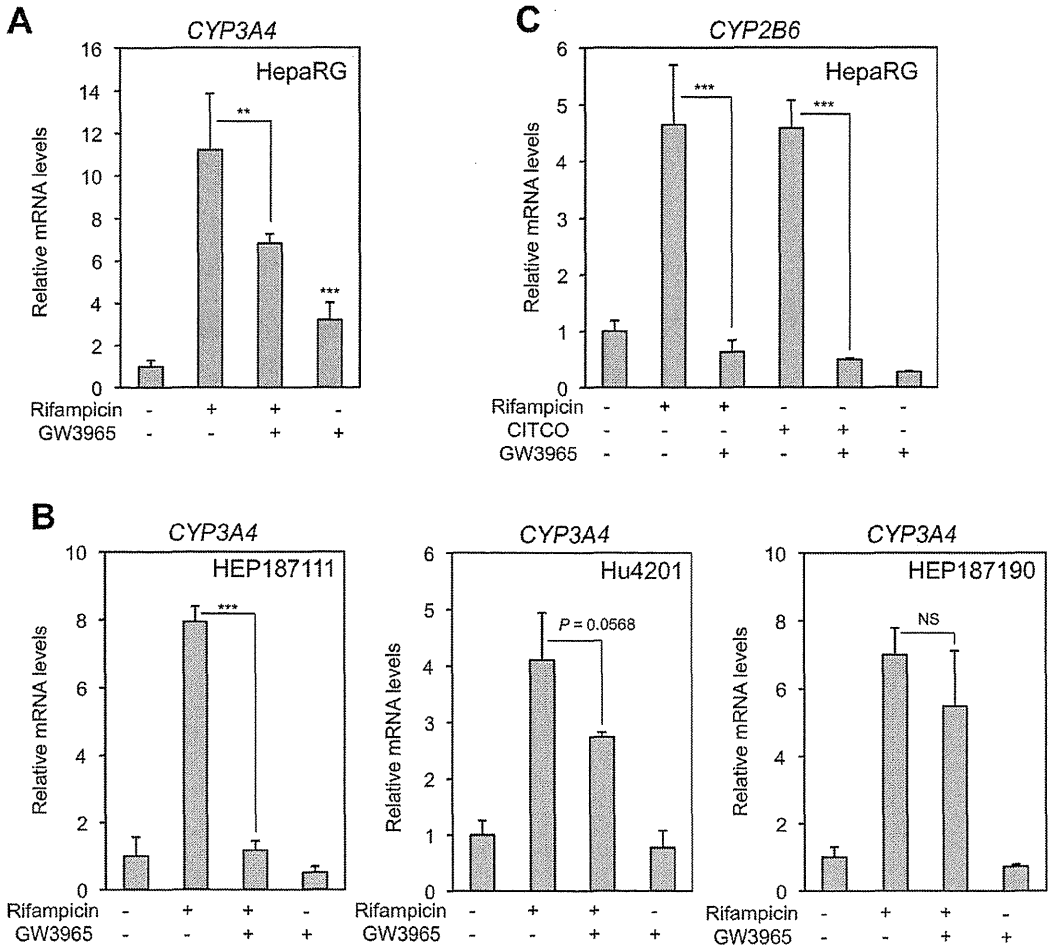

Fig. 4. Influences of GW3965 treatment on *CYP3A4* mRNA levels in human hepatocyte. Differentiated HepaRG cells (A and C) and primary human hepatocytes (B), cultured as described in Section 2, were treated with vehicle (0.2% DMSO), rifampicin (10 μM) or CITCO (0.3 μM) in the absence or presence of GW3965 (2 μM) for 48 h. *CYP3A4*, *CYP2B6* and *ACTB* mRNA levels were determined as described in Section 2. The results are expressed as relative mRNA levels to those in vehicle-treated cells. Data are the mean ± SD (n = 3–4). Experiments with HepaRG cells were carried out twice and representative data from one experiment are shown. Student's t-test was performed between two groups indicated; $^{**}P < 0.01$; $^{***}P < 0.001$; NS, not significant.

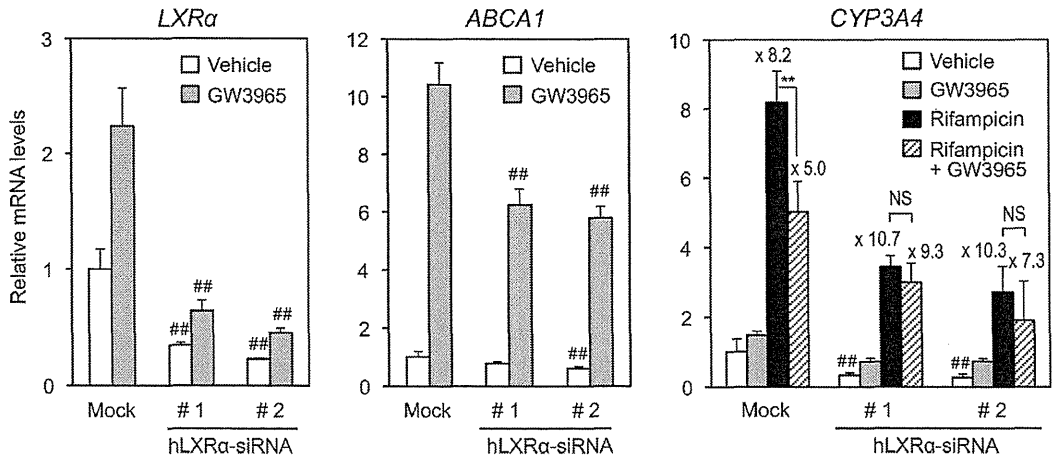

Fig. 5. Influence of hLXRα knockdown on GW3965- and/or rifampicin-induced changes in *CYP3A4* mRNA levels. HepaRG cells were transfected with control or hLXRα-targeting siRNA (#1 and #2) and were treated with vehicle (0.2% DMSO), GW3965 (2 μM) and/or rifampicin (10 μM) for 48 h as described in Section 2. mRNA levels were determined and are expressed as relative levels to those in control siRNA-transfected and vehicle-treated cells. Data are the mean ± SD (n = 4) of one representative experiment from 2 independent experiments. $^{\#\#}P < 0.01$, significantly different from the corresponding mock-transfected cells based on one-way ANOVA followed by Dunnett's post hoc test; NS, not significant. Student's t-test was performed between two groups indicated; $^{**}P < 0.01$.

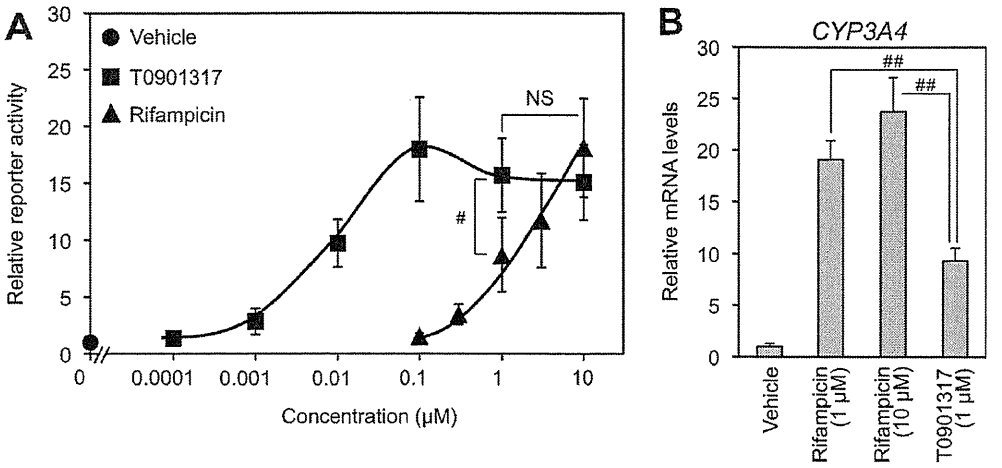

Fig. 6. Influence of T0901317 treatment on *CYP3A4* reporter activities and *CYP3A4* mRNA levels in HepaRG cells. (A) HepG2 cells (3×10^4 cells/well in 48-well plate) were transfected with p3A4 (0.5 μg), phRL-TK (0.025 μg) and pTarget-hPXR (0.1 μg). Twenty hours after transfection, the cells were treated with rifampicin (0.1–10 μM) or T0901317 (0.0001–10 μM) for 48 h, and reporter activities were measured. Firefly luciferase activities were normalized with *Renilla* luciferase activities. Data are expressed as relative activities to those in vehicle-treated cells. Data are the mean ± SD ($n = 4$) of one representative experiment from 3 independent experiments. (B) Differentiated HepaRG cells, cultured as described in Section 2, were treated with vehicle (0.1% DMSO), rifampicin (1 or 10 μM) or T0901317 (1 μM) for 48 h. *CYP3A4* and *ACTB* mRNA levels were determined as described in Section 2. The results are expressed as relative mRNA levels to those in the vehicle-treated cells. Data are the mean ± SD ($n = 4$). Experiments with HepaRG cells were carried out twice and representative data from one experiment are shown. $^{\#}P < 0.05$; $^{\#\#}P < 0.01$, significantly different from the T0901317 (1 μM)-treated cells based on one-way ANOVA followed by Dunnett's post hoc test; NS, not significant.

was attenuated by GW3965 co-treatment, as observed in Fig. 4A. On the other hand, GW3965 co-treatment barely affected the rifampicin-induced increase in *CYP3A4* mRNA levels in the cells transfected with *hLXRα*-siRNA (compare closed and hatched bars for each siRNA).

3.6. Comparison of T0901317 with rifampicin in CYP3A4 reporter assay and CYP3A4 induction in HepaRG cells

Results shown above suggest the inhibitory effects of hLXRα agonist for the hPXR-mediated *CYP3A4* expression. To investigate whether having a hLXRα agonistic activity might influence on the CYP3A4 induction in human hepatocytes by hPXR agonists, we compared the characteristics of rifampicin, a strong hPXR ligand, and T0901317, the hPXR/hLXRα dual agonist, in the PXR-based *CYP3A4* reporter assays and CYP3A4 induction assays with HepaRG cells. In reporter assays, treatment with 10 μM rifampicin or 1 μM T0901317 increased the *CYP3A4* reporter activities to a same extent (~18-fold, Fig. 6A). However, in HepaRG cells, treatment with 10 μM rifampicin greatly increased *CYP3A4* mRNA levels more than with 1 μM T0901317 treatment (Fig. 6B). Furthermore, treatment with 1 μM rifampicin was less effective in the PXR-dependent *CYP3A4* reporter assay than with 1 μM T0901317 (Fig. 6A) while it increased *CYP3A4* mRNA levels in HepaRG cells much more than T0901317 (1 μM) treatment (Fig. 6B). These results indicate that T0901317 is a stronger agonist of hPXR than rifampicin at the same concentration, but it induces less CYP3A4 in human hepatocytes than rifampicin.

4. Discussion

In this study, we have demonstrated unique dual roles of hLXRα in the expression of *CYP3A4*: ligand-activated hLXRα transactivates *CYP3A4* expression but suppresses the hPXR-dependent transcription of *CYP3A4*. Reporter assays using various deleted and mutated *CYP3A4* constructs and EMSAs have indicated that hLXRα transactivats *CYP3A4* through known hPXR-responsive elements, dNR1 and eNR3A4 (Fig. 2), showing that hLXRα and hPXR share binding motifs. We also found in reporter assays that the hPXR-dependent *CYP3A4* transactivation was attenuated by co-activation of hLXRα (Fig. 3A and B). Consistently, in HepaRG cells and human hepatocytes co-treatment with the hLXRα ligand GW3965 drastically reduced the hPXR-mediated increase in *CYP3A4* mRNA levels (Fig. 4A and B). The inhibitory effects of hLXRα on the hPXR-mediated *CYP3A4* expression were almost completely abolished by the knockdown of *hLXRα* in HepaRG cells (Fig. 5A). Taken together, our present results strongly suggest that the sterol-sensitive hLXRα is involved in the *CYP3A4* expression in human hepatocytes as a both positive and negative regulator.

Hepatic *CYP3A4* mRNA, protein and activity levels show large inter-individual variations in humans [28,29]. The reason for this variation remains unclear at present, but it seems that variations in the regulatory factors rather than the genetic polymorphism of the *CYP3A4* gene largely contribute to this [28,30]. In fact, several reports have demonstrated positive correlations between hepatic mRNA levels of *CYP3A4* and those for various transcription factors, including PXR, CAR, HNF4α, and FOXA2 [31–34]. Moreover, people are exposed to the PXR and CAR activators derived from pharmaceutical drugs, food and environmental contaminants at various levels in daily life, which also influences *CYP3A4* expression levels. Our present results suggest that LXRα is another positive regulator for the constitutive expression of *CYP3A4* in human livers. Given that LXRα is activated by various cholesterol metabolites (i.e. oxysterols), the amounts of cholesterol intake and metabolites formed may affect *CYP3A4* expression levels. Interestingly, we have recently demonstrated in mice that reduced intake of dietary cholesterol decreases hepatic *Cyp3a11* expression levels [20]. Thus, it is of great interest to investigate the association of *CYP3A4* expression levels with the activity and expression levels of LXRα as well as the genetic polymorphism of *NR1H3* (encoding hLXRα) in future studies.

We have found that the ligand-activated hLXRα suppresses the hPXR-mediated *CYP3A4* expression in both reporter assays (Fig. 3) and qRT-PCR analyses using human hepatocytes (Fig. 4). The precise mechanism underlying this phenomenon remains unclear, but these results have brought us a new insight into the CYP3A4 induction in terms of drug-drug interactions and drug development. There are large inter-individual variations in the responsiveness to PXR agonists in terms of CYP3A4 induction, as

observed in this study (Fig. 4B), and the influence of the LXRα ligand co-treatment on the rifampicin induction of CYP3A4 varied among 3 lots of hepatocytes (Fig. 4B). These results suggest that the LXRα activation level might be one of the determinants for the extent of xenobiotic-mediated CYP3A4 induction as well as basal CYP3A4 expression level in human livers.

Moreover, our results strongly suggest that a dual ligand of hLXRα/hPXR has a lower ability to induce *CYP3A4* expression than a pure hPXR ligand even if those two compounds have similar ability to activate hPXR, based on the results of the comparison between rifampicin and T0901317 in reporter assays and analysis of mRNA levels in HepaRG cells (Fig. 6). This implies that if a compound of interest activates hLXRα, its capability of inducing CYP3A4 in human livers cannot be estimated by a PXR-based reporter assays, which is often used to screen CYP3A4 inducers. In turn, this may indicate that PXR-mediated strong CYP3A4 induction in vivo can be avoided by conferring the ability to activate LXRα on a drug candidate.

qRT-PCR analyses of *CYP2B6* mRNA levels in HepaRG cells (Fig. 4C) suggest that LXRα is able to inhibit not only the PXR-mediated *CYP3A4* transactivation but also the PXR- and CAR-mediated *CYP2B6* transactivation. Since PXR, CAR and LXRα share RXRα as a binding partner, we anticipated that the mechanism underlying this phenomenon involved RXRα competition. However, the inhibitory effect of hLXRα was observed even when hRXRα was overexpressed (Fig. 3C). These results suggest that RXRα is not responsible for this phenomenon. Because PXR and LXRα share responsive elements of *CYP3A4* and other promoter regions, and coactivators, although further studies are needed, the hLXRα-mediated suppression of the hPXR/hCAR-induced expression of *CYP3A4* and *CYP2B6* might be caused by competition at the binding motifs in the promoter regions and/or competition for their coactivators by these nuclear receptors. In fact, some studies on the coactivator competition by two nuclear receptors have been reported [35–38]. Min et al. showed that CAR inhibited estrogen receptor-mediated transcription by competing for p160 coactivators, steroid receptor coactivator-1 and glucocorticoid receptor interacting protein-1. Saini et al. reported that ligand-free PXR inhibited the ligand-independent interaction between CAR and steroid receptor coactivator-1, resulting in the reduction of CAR-mediated expression of multidrug resistance associated protein 2. Miao et al. studied crosstalk between CAR and HNF-4 and suggest that CAR inhibits HNF-4-dependent transactivation of *CYP7A1* by competing with HNF-4 for coactivators, glucocorticoid receptor interacting protein-1 and peroxisome proliferator-activated receptor-γ coactivator-1α. Wada et al. revealed the mutual suppression of transcriptional activity between LXR and retinoid-related orphan receptor α, and indicate that coactivator competition might be a plausible mechanism for this crosstalk.

LXRα plays a key role in the cholesterol homeostasis through regulating the expression of numbers of genes involved in cholesterol uptake, transport and metabolism. Therefore, our present findings on the association of hLXRα with the *CYP3A4* expression suggest that CYP3A4 plays a role in the cholesterol homeostasis at least in the liver. In accordance with this idea, a couple of reports have demonstrated that CYP3A4 catalyzes the 4β-hydroxylation of cholesterol [12,19]. Interestingly, the metabolite 4β-hydroxycholeserol is an LXRα ligand, suggesting a feed-forward regulation of cholesterol metabolism through CYP3A4 and LXRα. Moreover, we have recently demonstrated in mice that hepatic *Cyp3a11* expression is down-regulated by reduced intake of dietary cholesterol through a mechanism involving SREBP-2, another cholesterol-sensing transcription factor [20]. Also, in AML12 cells, immortalized mouse hepatocytes, the addition of cholesterol and 25-hydroxycholesterol to the culture medium increased *Cyp3a11* mRNA levels (Yoshinari et al., unpublished results). These results obtained in mice strongly indicate that the hepatic *Cyp3a11* expression is tightly regulated by cellular sterol levels. Based on these reports and findings, several questions have been raised: Is SREBP-2 also involved in the regulation of *CYP3A4* expression? Does the amount of cholesterol intake affect the hepatic *CYP3A4* expression levels in humans in vivo? Is dyslipidemia such as fatty liver and hypercholesterolemia associated with the hepatic *CYP3A4* expression in humans? Or does induction or inhibition of CYP3A4 affect cholesterol homeostasis in humans? Answering these questions in future studies will reveal the role of CYP3A4 in the cholesterol homeostasis in humans as well as the physiological relevance of the hLXRα-mediated regulation of *CYP3A4* expression.

Acknowledgements

This study was supported in part by The Mochida Memorial Foundation for Medical and Pharmaceutical Research, The Japan Research Foundation for Clinical Pharmacology and a grant form Ministry of Health, Labour and Welfare of Japan. These funding sources played no role in study design; in the collection, analysis and interpretation of data; in the writing of the report; and in the decision to submit the paper for publication.

References

[1] Cholerton S, Daly AK, Idle JR. The role of individual human cytochromes P450 in drug metabolism and clinical response. Trends Pharmacol Sci 1992;13:434–9.
[2] Shimada T, Yamazaki H, Mimura M, Inui Y, Guengerich FP. Interindividual variations in human liver cytochrome P-450 enzymes involved in the oxidation of drugs, carcinogens and toxic chemicals: studies with liver microsomes of 30 Japanese and 30 Caucasians. J Pharmacol Exp Ther 1994;270:414–23.
[3] Williams JA, Hyland R, Jones BC, Smith DA, Hurst S, Goosen TC, et al. Drug–drug interactions for UDP-glucuronosyltransferase substrates: a pharmacokinetic explanation for typically observed low exposure (AUCi/AUC) ratios. Drug Metab Dispos 2004;32:1201–8.
[4] Paine MF, Hart HL, Ludington SS, Haining RL, Rettie AE, Zeldin DC. The human intestinal cytochrome P450 pie. Drug Metab Dispos 2006;34:880–6.
[5] Michalets EL. Update: clinically significant cytochrome P-450 drug interactions. Pharmacotherapy 1998;18:84–112.
[6] Wolbold R, Klein K, Burk O, Nussler AK, Neuhaus P, Eichelbaum M, et al. Sex is a major determinant of CYP3A4 expression in human liver. Hepatology 2003;38:978–88.
[7] Bertilsson G, Heidrich J, Svensson K, Asman M, Jendeberg L, Sydow-Backman M, et al. Identification of a human nuclear receptor defines a new signaling pathway for CYP3A induction. Proc Natl Acad Sci USA 1998;95:12208–13.
[8] Blumberg B, Sabbagh Jr W, Juguilon H, Bolado Jr J, van Meter CM, Ong ES, et al. SXR, a novel steroid and xenobiotic-sensing nuclear receptor. Genes Dev 1998;12:3195–205.
[9] Lehmann JM, McKee DD, Watson MA, Willson TM, Moore JT, Kliewer SA. The human orphan nuclear receptor PXR is activated by compounds that regulate CYP3A4 gene expression and cause drug interactions. J Clin Invest 1998;102:1016–23.
[10] Goodwin B, Hodgson E, Liddle C. The orphan human pregnane X receptor mediates the transcriptional activation of CYP3A4 by rifampicin through a distal enhancer module. Mol Pharmacol 1999;56:1329–39.
[11] Toriyabe T, Nagata K, Takada T, Aratsu Y, Matsubara T, Yoshinari K, et al. Unveiling a new essential cis element for the transactivation of the CYP3A4 gene by xenobiotics. Mol Pharmacol 2009;75:677–84.
[12] Bodin K, Bretillon L, Aden Y, Bertilsson L, Broome U, Einarsson C, et al. Antiepileptic drugs increase plasma levels of 4beta-hydroxycholesterol in humans: evidence for involvement of cytochrome p450 3A4. J Biol Chem 2001;276:38685–89.
[13] Kanebratt KP, Diczfalusy U, Backstrom T, Sparve E, Bredberg E, Bottiger Y, et al. Cytochrome P450 induction by rifampicin in healthy subjects: determination using the Karolinska cocktail and the endogenous CYP3A4 marker 4beta-hydroxycholesterol. Clin Pharmacol Ther 2008;84:589–94.
[14] Josephson F, Bertilsson L, Bottiger Y, Flamholc L, Gisslen M, Ormaasen V, et al. CYP3A induction and inhibition by different antiretroviral regimens reflected by changes in plasma 4beta-hydroxycholesterol levels. Eur J Clin Pharmacol 2008;64:775–81.
[15] Araya Z, Wikvall K. 6alpha-hydroxylation of taurochenodeoxycholic acid and lithocholic acid by CYP3A4 in human liver microsomes. Biochim Biophys Acta 1999;1438:47–54.
[16] Bodin K, Lindbom U, Diczfalusy U. Novel pathways of bile acid metabolism involving CYP3A4. Biochim Biophys Acta 2005;1687:84–93.

[17] Deo AK, Bandiera SM. Identification of human hepatic cytochrome p450 enzymes involved in the biotransformation of cholic and chenodeoxycholic acid. Drug Metab Dispos 2008;36:1983–91.
[18] Honda A, Salen G, Matsuzaki Y, Batta AK, Xu G, Leitersdorf E, et al. Side chain hydroxylations in bile acid biosynthesis catalyzed by CYP3A are markedly up-regulated in Cyp27−/− mice but not in cerebrotendinous xanthomatosis. J Biol Chem 2001;276:34579–85.
[19] Honda A, Miyazaki T, Ikegami T, Iwamoto J, Maeda T, Hirayama T, et al. Cholesterol 25-hydroxylation activity of CYP3A. J Lipid Res 2011;52:1509–16.
[20] Inoue S, Yoshinari K, Sugawara M, Yamazoe Y. Activated sterol regulatory element-binding protein-2 suppresses hepatocyte nuclear factor-4-mediated Cyp3a11 expression in mouse liver. Mol Pharmacol 2011;79:148–56.
[21] Lu TT, Repa JJ, Mangelsdorf DJ. Orphan nuclear receptors as eLiXiRs and FiXeRs of sterol metabolism. J Biol Chem 2001;276:37735–38.
[22] Janowski BA, Willy PJ, Devi TR, Falck JR, Mangelsdorf DJ. An oxysterol signalling pathway mediated by the nuclear receptor LXR alpha. Nature 1996;383:728–31.
[23] Janowski BA, Grogan MJ, Jones SA, Wisely GB, Kliewer SA, Corey EJ, et al. Structural requirements of ligands for the oxysterol liver X receptors LXRalpha and LXRbeta. Proc Natl Acad Sci USA 1999;96:266–71.
[24] Willy PJ, Umesono K, Ong ES, Evans RM, Heyman RA, Mangelsdorf DJLXR. a nuclear receptor that defines a distinct retinoid response pathway. Genes Dev 1995;9:1033–45.
[25] Araki K, Watanabe K, Yamazoe Y, Yoshinari K. Liver X receptor alpha bidirectionally transactivates human CYP1A1 and CYP1A2 through two cis-elements common to both genes. Toxicol Lett 2012;215:16–24.
[26] Yoshinari K, Yoda N, Toriyabe T, Yamazoe Y. Constitutive androstane receptor transcriptionally activates human CYP1A1 and CYP1A2 genes through a common regulatory element in the 5′-flanking region. Biochem Pharmacol 2010;79:261–9.
[27] Wang H, Negishi M. Transcriptional regulation of cytochrome p450 2B genes by nuclear receptors. Curr Drug Metab 2003;4:515–25.
[28] Lamba JK, Lin YS, Schuetz EG, Thummel KE. Genetic contribution to variable human CYP3A-mediated metabolism. Adv Drug Deliv Rev 2002;54:1271–94.
[29] Wortham M, Czerwinski M, He L, Parkinson A, Wan YJ. Expression of constitutive androstane receptor, hepatic nuclear factor 4 alpha, and P450 oxidoreductase genes determines interindividual variability in basal expression and activity of a broad scope of xenobiotic metabolism genes in the human liver. Drug Metab Dispos 2007;35:1700–10.
[30] Schuetz EG. Lessons from the CYP3A4 promoter. Mol Pharmacol 2004;65:279–81.
[31] Pascussi JM, Drocourt L, Gerbal-Chaloin S, Fabre JM, Maurel P, Vilarem MJ. Dual effect of dexamethasone on CYP3A4 gene expression in human hepatocytes. Sequential role of glucocorticoid receptor and pregnane X receptor. Eur J Biochem 2001;268:6346–58.
[32] Chang TK, Bandiera SM, Chen J. Constitutive androstane receptor and pregnane X receptor gene expression in human liver: interindividual variability and correlation with CYP2B6 mRNA levels. Drug Metab Dispos 2003;31:7–10.
[33] Lamba V, Panetta JC, Strom S, Schuetz EG. Genetic predictors of interindividual variability in hepatic CYP3A4 expression. J Pharmacol Exp Ther 2010;332:1088–99.
[34] Tegude H, Schnabel A, Zanger UM, Klein K, Eichelbaum M, Burk O. Molecular mechanism of basal CYP3A4 regulation by hepatocyte nuclear factor 4alpha: evidence for direct regulation in the intestine. Drug Metab Dispos 2007;35:946–54.
[35] Min G, Kim H, Bae Y, Petz L, Kemper JK. Inhibitory cross-talk between estrogen receptor (ER) and constitutively activated androstane receptor (CAR). CAR inhibits ER-mediated signaling pathway by squelching p160 coactivators. J Biol Chem 2002;277:34626–33.
[36] Saini SP, Mu Y, Gong H, Toma D, Uppal H, Ren S, et al. Dual role of orphan nuclear receptor pregnane X receptor in bilirubin detoxification in mice. Hepatology 2005;41:497–505.
[37] Miao J, Fang S, Bae Y, Kemper JK. Functional inhibitory cross-talk between constitutive androstane receptor and hepatic nuclear factor-4 in hepatic lipid/glucose metabolism is mediated by competition for binding to the DR1 motif and to the common coactivators, GRIP-1 and PGC-1alpha. J Biol Chem 2006;281:14537–46.
[38] Wada T, Kang HS, Angers M, Gong H, Bhatia S, Khadem S, et al. Identification of oxysterol 7alpha-hydroxylase (Cyp7b1) as a novel retinoid-related orphan receptor alpha (RORalpha) (NR1F1) target gene and a functional cross-talk between RORalpha and liver X receptor (NR1H3). Mol Pharmacol 2008;73:891–9.

Toxicology Letters 215 (2012) 16–24

Contents lists available at SciVerse ScienceDirect

Toxicology Letters

journal homepage: www.elsevier.com/locate/toxlet

Liver X receptor α bidirectionally transactivates human *CYP1A1* and *CYP1A2* through two cis-elements common to both genes☆

Kikuko Araki, Keisuke Watanabe, Yasushi Yamazoe, Kouichi Yoshinari*

Division of Drug Metabolism and Molecular Toxicology, Graduate School of Pharmaceutical Sciences, Tohoku University, 6-3 Aramaki-aoba, Aoba-ku, Sendai, Miyagi 980-8578, Japan

HIGHLIGHTS

- ► LXRα activation induced transactivation of both h*CYP1A1* and h*CYP1A2* simultaneously.
- ► LXRα-mediated transactivation of h*CYP1A1* and h*CYP1A2* is through two regions.
- ► LXRα/RXRα heterodimer binds to two ER8 motifs in the proximal promoter of h*CYP1A1*.
- ► LXRα synergistically transactivated h*CYP1A1* and h*CYP1A2* with AhR but not CAR.
- ► LXRα ligand increased h*CYP1A1* and h*CYP1A2* mRNA levels in a cell-specific manner.

ARTICLE INFO

Article history:
Received 31 July 2012
Received in revised form
24 September 2012
Accepted 26 September 2012
Available online xxx

Keywords:
Nuclear receptor
Drug metabolism
Bidirectional transcription
Reporter assay
Hepatocytes
LXRα

ABSTRACT

CYP1A1 and CYP1A2 are involved in both detoxification and metabolic activation of xenobiotics. Human *CYP1A1* (h*CYP1A1*) and h*CYP1A2* exist in a head-to-head orientation in chromosome 15 with the overlapping 5′-flanking region. We have recently reported that nuclear receptor constitutive androstane receptor (CAR), in addition to aryl hydrocarbon receptor, bidirectionally transactivates these genes through common motifs. In this study, we have investigated a role of liver X receptor α (LXRα), another liver-enriched nuclear receptor, in the expression h*CYP1A1* and h*CYP1A2*. In reporter assays with dual-reporter constructs containing their promoter region between two different reporter genes, LXRα simultaneously transactivated h*CYP1A1* and h*CYP1A2* through two regions, independent of aryl hydrocarbon receptor. In electrophoretic mobility shift assays, LXRα/retinoid X receptor α heterodimer bound to two ER8-type motifs found at around −520 and −460 of h*CYP1A1*. The former corresponds to the CAR-binding motif previously identified. Reporter assays using mutated constructs confirmed the critical roles of these motifs in the LXRα-mediated simultaneous transcription of h*CYP1A1* and h*CYP1A2*. h*CYP1A1* and h*CYP1A2* mRNA levels were increased in human hepatoma HuH-7 cells and human primary hepatocytes, respectively, after treatment with the LXRα ligand GW3965. Our results suggest that LXRα transactivates the expression of h*CYP1A1* and h*CYP1A2* through common two cis-elements.

1. Introduction

CYP1A1 and CYP1A2 are involved in both detoxification and metabolic activation of xenobiotics including procarcinogens, and also important for the metabolism of endogenous compounds such as estrogens (Badawi et al., 2001; Lee et al., 2003). These enzymes are highly inducible after exposure to polycyclic aromatic hydrocarbons such as 3-methylcholanthrene (3MC) and 2,3,7,8-tetrachlorodibenzo-*p*-dioxin. This induction results from the enhanced transcription of both genes through the ligand-activated aryl hydrocarbon receptor (AhR) (Denison and Nagy, 2003). In response to ligands, AhR binds to the cis-element termed xenobiotics-responsive element (XRE) in the 5′-flanking region of target genes to activate their transcription. Human *CYP1A1* (h*CYP1A1*) and h*CYP1A2* are located in a head-to-head orientation in chromosome 15 and share an about 23-kb 5′-flanking region. We have recently demonstrated that both genes share a common regulatory region and that the region from −460 to −1826 of h*CYP1A1* containing five XREs works bidirectionally for the AhR-mediated transcription of h*CYP1A1* and h*CYP1A2* (Ueda et al., 2006;

Abbreviations: LXR, liver X receptor; CAR, constitutive androstane receptor; RXR, retinoid X receptor; AhR, aryl hydrocarbon receptor; 24HC, 24(S)-hydroxycholesterol; 3MC, 3-methylcholanthrene; CITCO, 6-(4-chlorophenyl)imidazo[2,1-*b*][1,3]thiazole-5-carbaldehyde-O-(3,4-dichlorobenzyl)oxime; DMSO, dimethyl sulfoxide; SEAP, secreted alkaline phosphatase; EMSA, electrophoretic mobility shift assay; h, human; ER, everted repeat; DR, direct repeat; XRE, xenobiotic-responsive element.

☆ A part of the data in this manuscript was presented at the 17th North American Regional ISSX Meeting, October 16–20, 2011, Atlanta, GA, USA.

* Corresponding author. Tel.: +81 22 795 6828; fax: +81 22 795 6826.
E-mail address: yoshinari@m.tohoku.ac.jp (K. Yoshinari).

0378-4274/$ – see front matter © 2012 Elsevier Ireland Ltd. All rights reserved.
http://dx.doi.org/10.1016/j.toxlet.2012.09.021

Yoshinari et al., 2008). In addition, we have also found that constitutive androstane receptor (CAR), a xenobiotic-responsive nuclear receptor, transactivates h*CYP1A1* and h*CYP1A2* independent of AhR (Yoshinari et al., 2010). CAR heterodimerizes with retinoid X receptor α (RXRα), binds to an ER8 (everted repeat separated by 8 nucleotides)-type motif, located at around −520 of h*CYP1A1*, and transactivates both genes bidirectionally (Yoshinari et al., 2010). Thus, the mechanisms for the xenobiotic-induced transcription of h*CYP1A1* and h*CYP1A2* have been increasingly understood.

Liver X receptors α (LXRα) and LXRβ belong to the nuclear receptor superfamily. LXRα is highly expressed in the liver, intestine, brain and macrophages, while LXRβ is expressed ubiquitously (Lu et al., 2001). These receptors are activated by oxysterols including 4β-hydroxycholesterol and 24(S)-hydroxycholesterol (24HC) (Janowski et al., 1996) as well as high-affinity synthetic agonists such as GW3965 (Collins et al., 2002) and T0901317 (Repa et al., 2000; Schultz et al., 2000). Upon ligand binding, LXRs, as a heterodimer with RXR, bind to DR4 (direct repeat separated by 4 nucleotides)-type motifs found in the promoter regions of target genes to transactivate them (Willy et al., 1995). The target genes include those associated with lipid homeostasis, such as *CYP7A1*, *SREBP1*, *ABCA1 ABCG5* and *ABCG8* (Janowski et al., 1999; Lu et al., 2001). Recent reports suggest that LXRα is also involved in the expression of genes encoding drug-metabolizing enzymes such as mouse CYP3A11 (Gnerre et al., 2005) and human and mouse UGT1A3 (Verreault et al., 2006), and drug-transporters such as human OATP1B1 (Meyer Zu Schwabedissen et al., 2010) and MRP2 (Chisaki et al., 2009).

In the present study, we have investigated a possible involvement of LXRα in the transactivation of h*CYP1A1* and h*CYP1A2*. We have raised this possibility based on the following reasons: (1) LXRα, like CAR, is highly expressed in the liver and prefers DR4-type motifs as its binding sequences (Lu et al., 2001; Swales and Negishi, 2004; Willy et al., 1995); (2) LXRα is suggested to regulate the expression of genes associated with drug metabolism and disposition as mentioned above (Chisaki et al., 2009; Gnerre et al., 2005; Meyer Zu Schwabedissen et al., 2010; Verreault et al., 2006); (3) Treatment of mice with LXRα agonists (22(R)-hydroxycholesterol or GW3965), slightly but significantly increased hepatic *Cyp1a2* mRNA levels, although the authors concluded that LXRα effects on *Cyp1a2* expression was negligible (Gong et al., 2007); (4) Finally, recombinant CYP1A2 has been reported to catalyze the conversion of cholesterol to 4β-hydroxycholesterol, which is an LXRα agonist (Honda et al., 2011; Janowski et al., 1996). Using the dual-reporter system recently developed in our laboratory (Ueda et al., 2006), we here demonstrate that human LXRα is able to bidirectionally transactivate h*CYP1A1* and h*CYP1A2* through two cis-elements common to both genes.

2. Materials and methods

2.1. Materials

T4 polynucleotide kinase and restriction enzymes were purchased from New England BioLabs (Ipswich, MA). Poly(dI–dC) and [γ-^{32}P]ATP were purchased from GE Healthcare (Piscataway, NJ) and PerkinElmer (Waltham, MA), respectively. All other chemicals were of highest grade available purchased from Wako Pure Chemical Industries (Osaka, Japan) or Sigma–Aldrich (St. Louis, MO) unless otherwise mentioned. Oligonucleotide DNAs were commercially synthesized by Fasmac (Atsugi, Japan).

2.2. Plasmid DNA

Dual-reporter constructs used in Figs. 1 and 2, 6, 7 were prepared previously (Ueda et al., 2006; Yoshinari et al., 2010). A mutated construct, pd1AΔ-1827/-21975m was prepared previously (Yoshinari et al., 2008). pd1AΔ-1827/-21975dm was made by using QuikChange Lightning Site-Directed Mutagenesis Kit (Stratagene, La Jolla, CA) with the primers, 5′-GCGGGGGCGGGGCTGCCCCGTGGTTACATCCTTCCCGGGGTTACTGAG-3′ and 5′-CTCAGTAACCCCGGGAAGGATGTAACCACGGGGCAGCCCCGCCCCCGC-3′.

The hLXRα cDNA was amplified by PCR using KOD-FX (TOYOBO, Tokyo, Japan) and the primers, 5′-CAGAAAGAGATGTCCTTGTG-3′ and 5′-AACAGTCATTCGTGCACATC-3′, and inserted into pTargeT (Promega, Madison, WI) to obtain mammalian expression plasmid pT-hLXRα. The cDNA fragment obtained by digesting pT-hLXRα with MluI and NotI was inserted into the same restriction sites of pTNT (Promega) for in vitro synthesis. pTarget-hCAR, pTNT-hRXRα and pTNT-hCAR were reported previously (Yoshinari et al., 2010).

2.3. Cell culture and reporter assay

HuH-7 and HepG2 cells (RIKEN BioResource Center, Tsukuba, Japan) were cultured in Dulbecco's modified Eagle's medium supplemented with 10% heat-inactivated fetal bovine serum (Nichirei Biosciences, Tokyo, Japan), minimum essential medium nonessential amino acids (Invitrogen, Carlsbad, CA) and antibiotic–antimycotic (Invitrogen). Cells were seeded in 48-well plates (BD Biosciences, San Jose, CA) 24 h before transfection. Reporter construct and pTarget expression plasmid (empty, pTarget-hLXRα, pTarget-hCAR) were transfected using jetPEI (PolyPlus Transfection, Illkirch, France). phRL-tk Control Vector was cotransfected to normalize transfection efficiency. Eight hours after transfection, cells were treated with 10 μM 24HC (Biomol, Plymouth Meeting, PA), 0.3 μM 6-(4-chlorophenyl)imidazo[2,1-*b*][1,3]thiazole-5-carbaldehyde-O-(3,4-dichlorobenzyl)oxime (CITCO; MERCK, Darmstadt, Germany), 1 μM 3MC (Toronto Research Chemicals, North York, Ontario, Canada) and vehicle (0.1% dimethyl sulfoxide; DMSO) for 40 h in medium without fetal bovine serum. Subsequently, the cells were harvested, and luciferase and secreted alkaline phosphatase (SEAP) activities were determined as described previously (Yoshinari et al., 2010). Representative results out of 2 or 3 independent assays are presented.

2.4. Electrophoretic mobility shift assay (EMSA)

hLXRα and hRXRα were synthesized in vitro with the corresponding pTNT plasmid, using TNT SP6 Quick Coupled Transcription/Translation System (Promega). Control lysate was prepared using empty pTNT. The sequences of double-stranded oligonucleotides used are shown in 3A, 4A and B. EMSAs were performed as described previously (Yoshinari et al., 2010). Briefly, nuclear receptor-containing or control lysates were incubated with each ^{32}P-labeled probe in reaction mixture containing 10 mM Tris–HCl, pH 8.0, 5% glycerol, 100 mM KCl, 1 mM dithiothreitol and 1 mg of poly(dI–dC) for 30 min at room temperature. For competition assays, unlabeled probes were added to the reaction mixture. Protein–DNA complexes were separated on 4% non-denaturing polyacrylamide gel in 0.25× TBE buffer (22.5 mM Tris–HCl, 22.5 mM boric acid, 0.5 mM EDTA, pH 8.0) and detected with FLA-3000 image analyzer (FujiFilm, Tokyo, Japan).

2.5. Quantitative reverse transcription-PCR (qRT-PCR)

HuH-7 cells seeded in 24-well plate (2×10^5 cells/well) in Dulbecco's modified Eagle's medium/10% fetal bovine serum were treated with vehicle (0.1% DMSO), 10 μM 24HC, 1 μM T0901317 (Sigma–Aldrich), 2 μM GW3965 (Sigma–Aldrich) or 1 μM 3MC for 48 h. Human hepatocytes (Biopredic International, Rennes, France; lot HEP187190 and HEP187111), seeded and cultured as described previously (Yoshinari et al., 2010), were treated with vehicle (0.2% DMSO), 10 μM 24HC, 1 μM T0901317, 2 μM GW3965 or 0.3 μM CITCO for 48 h, refreshing the inducer-containing medium after the first 24 h. Total RNA was prepared from the cells using Sepasol reagent (Nacalai Tesque, Kyoto, Japan) for HuH-7 and HepG2 cells and SV Total RNA Isolation System (Promega) for human hepatocytes according to the manufacturers' manuals. Determination of h*CYP1A1* and h*CYP1A2* mRNA levels were carried out as described previously (Yoshinari et al., 2010) except that GoTaq qPCR Master Mix (Promega) was used for real-time PCR. Primer sequences for *GAPDH* were 5′-ACATCAAGAAGGTGGTGAAG-3′ and 5′-CCACCACCCTGTTGCTGTAG-3′.

2.6. Statistical analysis

Student's *t*-test (2 group comparison) and one-way ANOVA followed by Dunnett's test or Bonferroni's multiple comparison test as post hoc test (multiple group comparison) were performed with Prism software (ver. 4.0, GraphPad Software, San Diego, CA). A *P*-value less than 0.05 ($P < 0.05$) was considered as statistically significant.

3. Results

3.1. Transcriptional activation of both hCYP1A1 and hCYP1A2 by hLXRα

We first performed reporter assays using the dual-reporter system, which had been developed in our laboratory (Ueda et al., 2006). With this system, transcriptional activities of h*CYP1A1* and h*CYP1A2* are simultaneously determined as luciferase and SEAP activities, respectively. In a system using pd-1A1/1A2, a

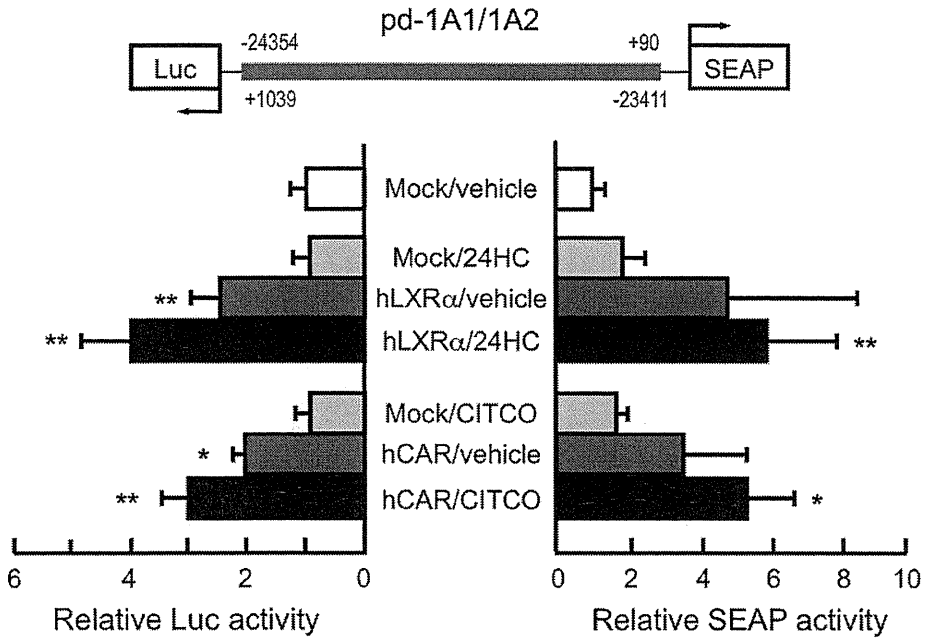

Fig. 1. Influence of hLXRα activation on the transcription of h*CYP1A1* and h*CYP1A2*. (A) Schematic structure of the dual reporter plasmid (pd-1A1/1A2) is shown on the top. The numbers above and below the plasmid represent the positions from the transcriptional starting points of h*CYP1A2* and h*CYP1A1*, respectively. (B) HuH-7 cells (3×10^4 cells in 48-well plate) were transfected with pd-1A1/1A2 (300 ng), phRL-tk (10 ng), and either control (mock) or nuclear receptor (hLXRα and hCAR) expression plasmid (20 ng). Eight hours after transfection, cells were treated with 10 μM 24HC, 0.3 μM CITCO or vehicle (0.1% DMSO) for 40 h, and reporter activities were measured. Firefly luciferase and SEAP activities normalized with *Renilla* luciferase activities are shown as ratios to those in control plasmid-transfected and vehicle-treated cells (Mock/vehicle). Data are shown as the mean ± S.D. ($n = 3$–4). Luc: luciferase. *$P < 0.05$, **$P < 0.01$ versus Mock/vehicle group (one-way ANOVA followed by Dunnett's post hoc test).

dual-reporter construct containing the whole 5′-flanking region (Fig. 1), co-transfection of hLXRα-expressing plasmid slightly increased both luciferase and SEAP activities in HuH-7 cells (Fig. 1). Treatment with the LXRα ligand, 24HC, further increased both activities of pd-1A1/1A2 to a similar extent with hCAR activation (Fig. 1). hLXRα activation also increased both reporter activities in HepG2 cells (data not shown). These results suggest that hLXRα simultaneously transactivates h*CYP1A1* and h*CYP1A2*.

3.2. Identification of hLXRα-responsive regions

To identify an hLXRα-responsive region(s), reporter assays were performed with various deletion constructs derived from pd-1A1/1A2 (Fig. 2A). Activation of hLXRα increased both luciferase and SEAP activities of pd-1A1/1A2, pd1AΔ-4618/-21975 and pd1AΔ-1827/-21975. But the deletion of nucleotides from −461 to −1826 of h*CYP1A1* resulted in the complete loss of the hLXRα-mediated increase in both reporter activities. These results suggested that the region from −461 to −1826 of h*CYP1A1* was responsible for the hLXRα-mediated transactivation of both h*CYP1A1* and h*CYP1A2*. Thus, we further investigated the hLXRα-responsive region using additional deletion constructs. As depicted in Fig. 2B, the deletion of nucleotides from −511 to −554 of h*CYP1A1*, which contains the CAR-responsive ER8 motif (termed $ER8_1$), reduced the hLXRα-mediated expression of both genes. Further deletion of nucleotides from −510 to −461 of h*CYP1A1* completely abolished the hLXRα-mediated expression of both genes. These results suggest that hLXRα transactivates both h*CYP1A1* and h*CYP1A2* simultaneously through two promoter regions, one from −511 to −554 of h*CYP1A1* and the other from −461 to −510 of h*CYP1A1*.

3.3. Identification of hLXRα/hRXRα heterodimer binding motifs

One of the LXRα-responsive regions that from −511 to −554 of h*CYP1A1*, contains the CAR-binding motif $ER8_1$ (Yoshinari et al., 2010). We thus investigated whether hLXRα/hRXRα heterodimer could bind to $ER8_1$ in EMSAs using various lengths of radiolabeled probes containing the AGGTCA half-site, one of the $ER8_1$ half-sites (Fig. 3A). As shown in Fig. 3B, hLXRα/hRXRα heterodimer strongly bound to P6 and weakly to P5 and P4, all of which contained $ER8_1$, while the binding of the heterodimer to P3, P2 and P1 was trivial. hLXRα or hRXRα alone did not bind to P6 (Fig. 3B). These results suggested that hLXRα binds to $ER8_1$ as a heterodimer with hRXRα like hCAR. Consistently, hLXRα/hRXRα heterodimer did not bind to probes P6m1, P6m2 and P6dm, which contained a mutation(s) in either half-site or both (Fig. 3C). In addition, the binding of the heterodimer to P6 was strongly competed by unlabeled P6 itself and weakly by shorter probes P5, P4, P3, P2 and P1 (data not shown).

The results of reporter assays suggested the presence of another hLXRα-responsive element at around −460 of h*CYP1A1*. To identify the responsive element, we carried out EMSAs with oligonucleotides probes shown in Fig. 4A. As shown in Fig. 4C, hLXRα/hRXRα heterodimer bound to P70 containing the oligonucleotides from −451 to −520 of h*CYP1A1*. Neither hLXRα nor hRXRα alone bound to P70 (Supplementary Fig. s1A). Fifty-fold excess of unlabeled P70 and P70A, but not P70B and P70C, abolished the binding of the hLXRα/hRXRα heterodimer to P70 (Fig. 4C). These results suggested that the heterodimer binds to the region from −451 to −487 of h*CYP1A1*. Scrutinizing the sequence of the region, we found an ER8-type motif (termed $ER8_2$) at around −460 of h*CYP1A1* (Fig. 4B). We thus investigated whether hLXRα/hRXRα heterodimer could bind to this motif using EMSAs with PAm1, PAm2 and PAdm, containing a mutation(s) in either half-site or both of $ER8_2$ (Fig. 4B). As results, hLXRα/hRXRα heterodimer did not bind to PAm1 and PAdm, while faint binding to PAm2 was observed

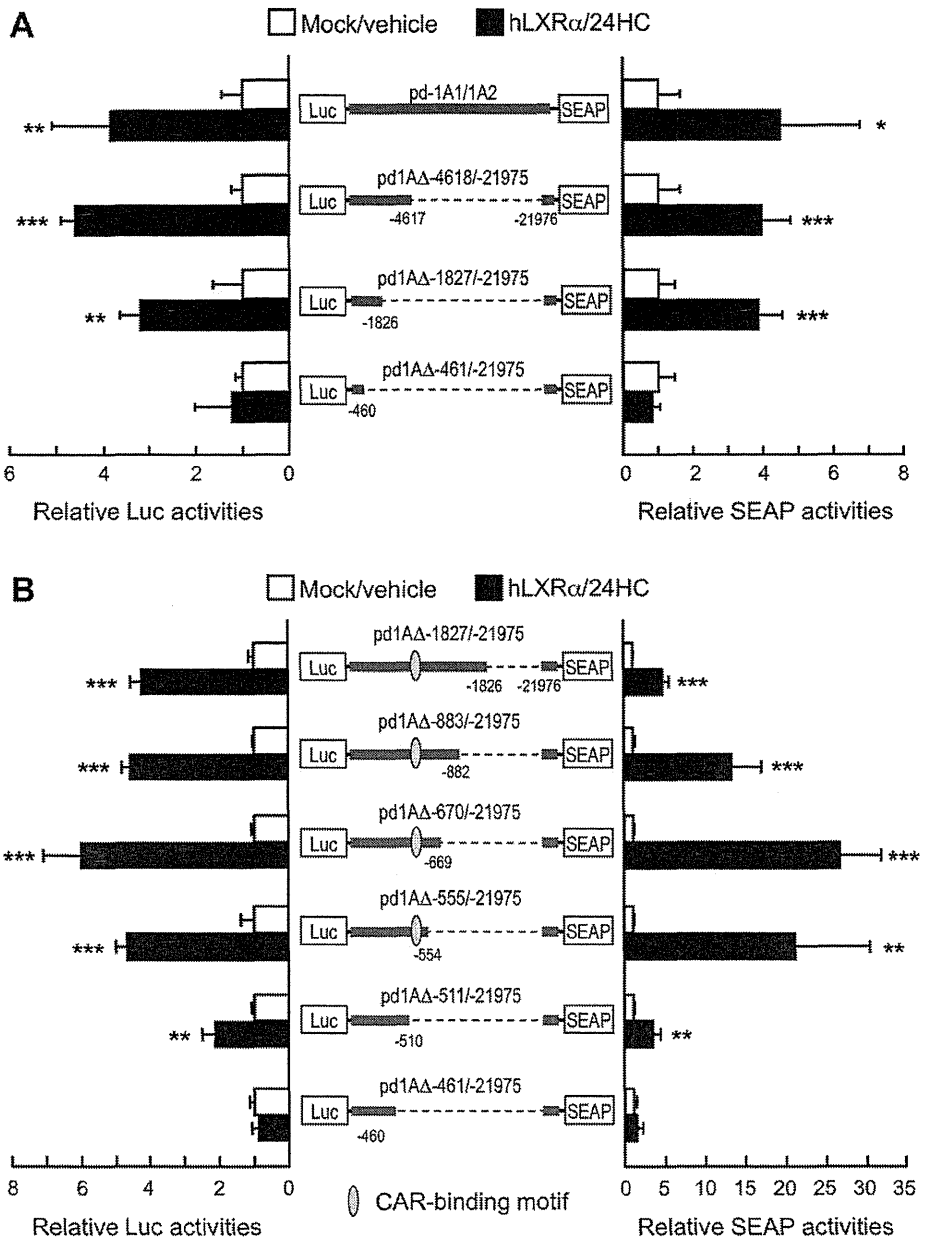

Fig. 2. Identification of hLXRα-responsive region(s) of h*CYP1A1* and h*CYP1A2*. (A and B) Schematic structures of the reporter plasmids used are shown in the middle. Reporter assays were performed as in Fig. 1. Normalized reporter activities in control plasmid-transfected and vehicle-treated cells are set at one for each reporter construct. Data are shown as the mean ± S.D. ($n = 3–4$). *$P < 0.05$, **$P < 0.01$, ***$P < 0.001$ versus corresponding Mock/vehicle groups (Student's *t*-test).

(Fig. 4D). Consistently, the shifted complex of hLXRα/hRXRα heterodimer with P70A was competed by P70A itself and very weakly by PAm2, but not by PAm1 and PAdm (Supplementary Fig. s1B).

3.4. Role of two ER8-type motifs in the hLXRα-mediated bidirectional transactivation of hCYP1A1 and hCYP1A2

To examine whether $ER8_1$ and $ER8_2$ were essential for the hLXRα-mediated transactivation of both h*CYP1A1* and h*CYP1A2*, we carried out reporter assays with wild-type and mutated constructs (Fig. 5). When a mutated construct lacking the functional $ER8_1$ motif was used, hLXRα-responsiveness of both genes was much weaker than that with a wild-type construct. The introduction of mutations into both $ER8_1$ and $ER8_2$ completely abolished the hLXRα-mediated transcription of these genes. These results suggest that two ER8-type motifs, $ER8_1$ and $ER8_2$, cooperate on the hLXRα-mediated bidirectional transactivation of h*CYP1A1* and h*CYP1A2*.

3.5. Changes in mRNA levels of hCYP1A1 and hCYP1A2 after treatment with LXRα ligands

To investigate whether LXRα activation increases h*CYP1A1* and h*CYP1A2* mRNA levels in hepatocytes, HuH-7 cells and primary human hepatocytes were treated with LXRα ligands and qRT-PCR was performed. As shown in Fig. 6A, treatment with GW3965 or T0901317 increased h*CYP1A1* but not h*CYP1A2* mRNA levels in HuH-7 cells. Similar results were obtained with HepG2 cells (data not shown). On the other hand, LXRα ligand GW3965 increased

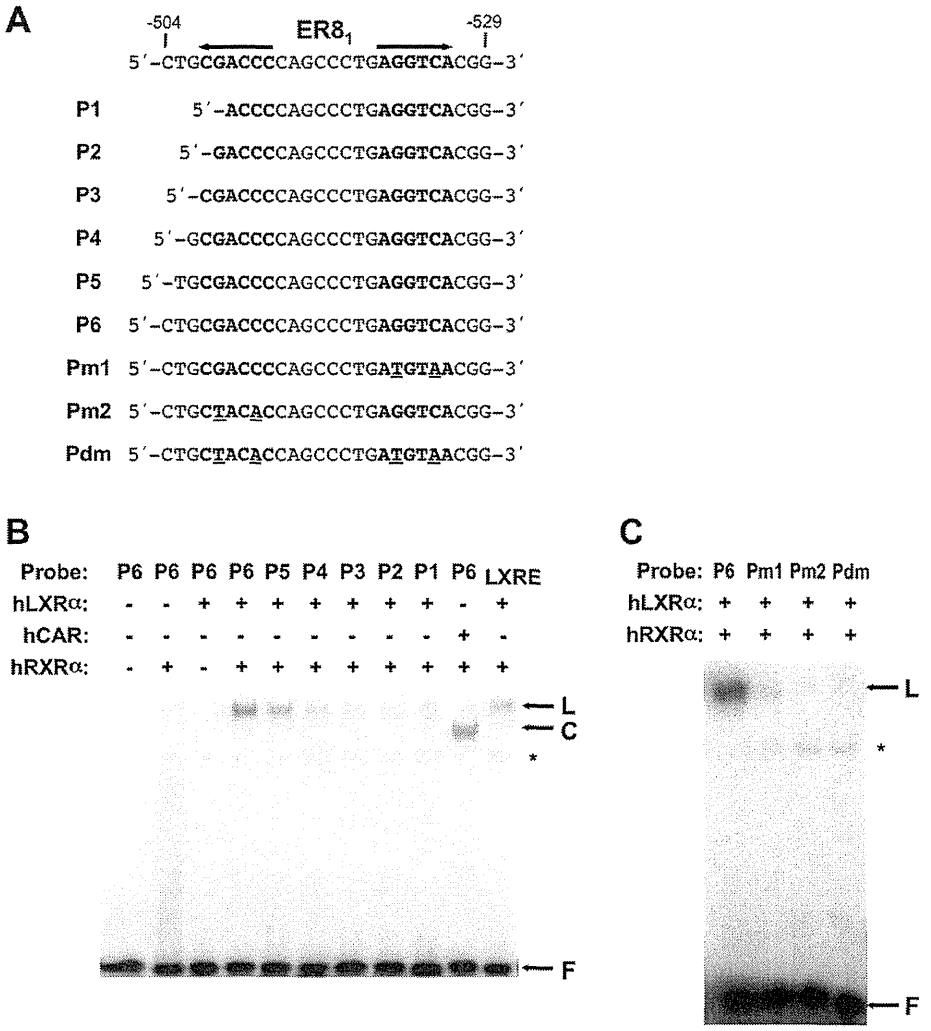

Fig. 3. Identification of a hLXRα/hRXRα heterodimer binding motif at around −520 of h*CYP1A1*. (A) Sequences of the oligonucleotide probes used are shown. Underlined nucleotides represent mutated ones. ER8$_1$ motif is indicated with bold letters and arrows. (B and C) EMSAs were carried out with radiolabeled probes and in vitro synthesized proteins as indicated. Probe LXRE contains the DR4 motif from rat *Cyp7a1* (Chiang et al., 2001). Asterisk indicates non-specific bindings. L; hLXRα–hRXRα-probe complex, C; hCAR–hRXRα-probe complex, F; free probe.

h*CYP1A2* but not h*CYP1A1* mRNA levels in primary human hepatocytes (Fig. 6B).

3.6. Co-regulation of hCYP1A1 and hCYP1A2 by LXRα, AhR and CAR

Recently, we have shown that the XRE cluster, a region from −461 to −1826 of h*CYP1A1*, is commonly essential for the AhR-mediated transcription of both h*CYP1A1* and h*CYP1A2*. The fact that ER8$_1$ and ER8$_2$ are located within the XRE cluster has raised a possibility of functional cooperation between LXRα and AhR in the expression of both h*CYP1A1* and h*CYP1A2*. This possibility was investigated in reporter assays. Both luciferase and SEAP activities of pd-1A1/1A2 were increased to a similar extent (25- to 30-fold) after treatment with the AhR ligand 3MC (Fig. 7). In the presence of 3MC at the concentration (1 μM) where maximum 3MC-dependent increases in reporter activities were observed (Supplementary Fig. s2), hLXRα activation further increased both reporter activities (Fig. 7A). These results suggest that hLXRα transactivates h*CYP1A1* and h*CYP1A2* independent of AhR. In contrast, no such synergistic transactivation of h*CYP1A1* and h*CYP1A2* was observed with LXRα and CAR, since both reporter activities after simultaneous activation of hLXRα and CAR were similar to those after hLXRα activation alone (Fig. 7B).

4. Discussion

In this study, we have investigated a possible involvement of hLXRα in the gene expression of h*CYP1A1* and h*CYP1A2*. With dual-reporter constructs, containing the whole or partially deleted h*CYP1A* promoter sequences between two different reporter genes, we have found that hLXRα transactivates the expression of both genes through two regions (from −554 to −511 and from −510 to −461 of h*CYP1A1*). EMSAs demonstrated that hLXRα binds to two ER8-type motifs (ER8$_1$ and ER8$_2$) found at around −520 and −460 of h*CYP1A1* as a heterodimer with RXRα. ER8$_1$ corresponds to the CAR-binding motif that we found previously (Yoshinari et al., 2010). The critical roles of these two ER8 motifs in the hLXRα-mediated transcription of h*CYP1A1* and h*CYP1A2* were confirmed by reporter assays using reporter constructs in which these motifs were individually or simultaneously mutated. These results suggest that the two ER8 motifs function as hLXRα-responsive elements for the bidirectional transactivation of both h*CYP1A1* and h*CYP1A2* and that

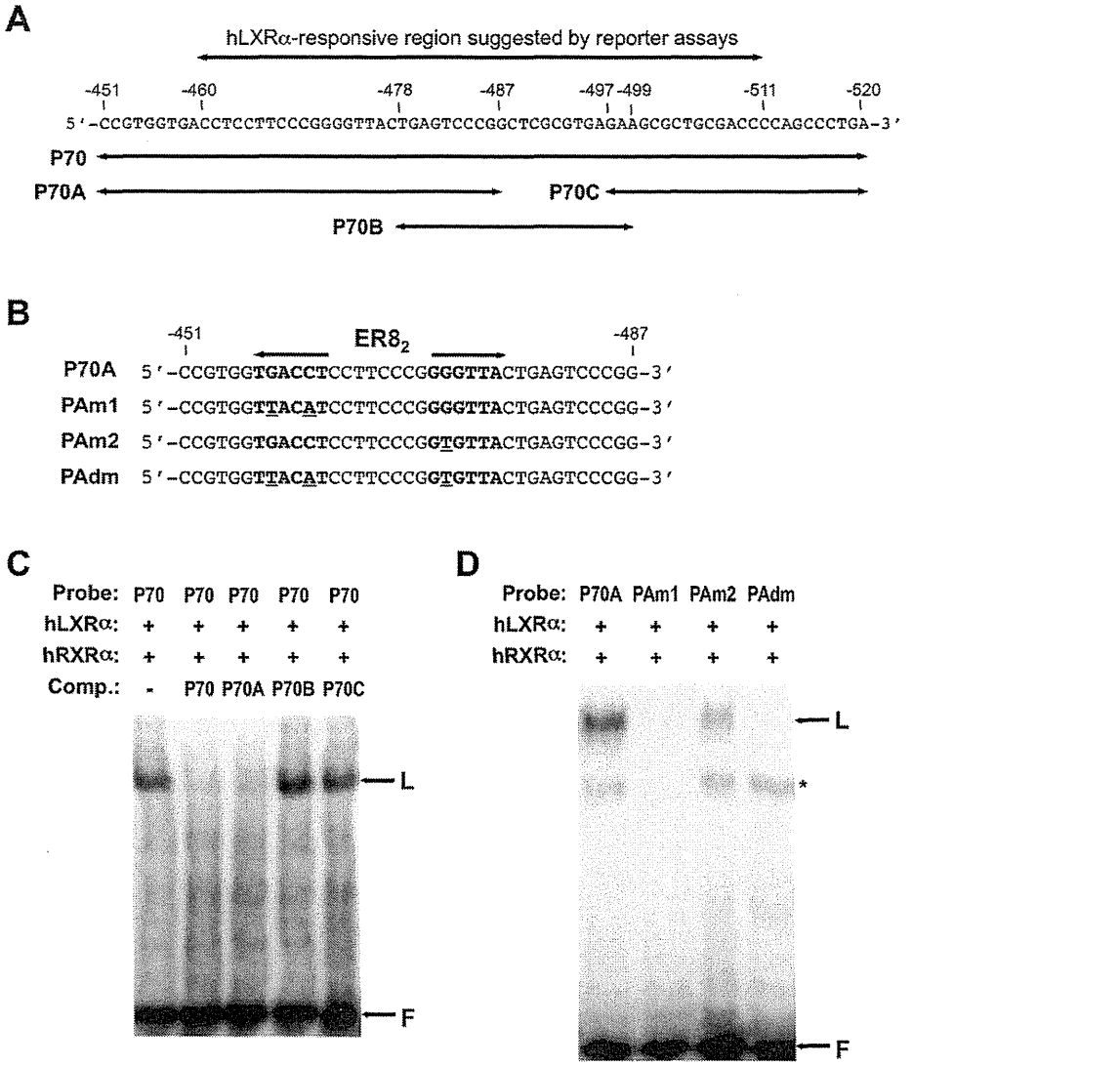

Fig. 4. Identification of a hLXRα/hRXRα heterodimer binding motif at around −460 of h*CYP1A1*. (A and B) Sequences of the oligonucleotide probes used are shown. Underlined nucleotides represent mutated ones. (C and D) EMSAs were carried out as in Fig. 3. Asterisk indicates non-specific bindings. L, hLXRα–hRXRα-probe complex; F, free probe; comp.; 50-fold excess non-labeled probe.

LXRα is a new member of transcription factors that control the expression levels of both h*CYP1A1* and h*CYP1A2*.

In contrast to the reporter assays, the influences of LXRα ligand treatment on h*CYP1A1* and h*CYP1A2* mRNA levels were cell type-dependent. In hepatoma cells such as HuH-7 and HepG2 cells, h*CYP1A1*, but not h*CYP1A2*, mRNA levels were increased in response to LXRα ligands. In contrast, h*CYP1A2*, but not h*CYP1A1*, mRNA levels were increased after LXRα ligand treatment in primary human hepatocytes. At this moment, the reason for the discrepancy remains unknown. It is well known that *CYP1A2* is highly expressed in adult livers of mammals and *CYP1A1* is barely expressed in the liver. In contrast, *CYP1A1*, but not *CYP1A2* is highly expressed in the extrahepatic tissues. In HuH-7 and HepG2 cells, both h*CYP1A1* and h*CYP1A2* are expressed. These facts suggest that an as-yet-unidentified factor(s) regulates the cell-specific expression of these genes. Such factor(s) may also influence the hLXRα-mediated expression of h*CYP1A1* and h*CYP1A2*.

The LXRα-responsive ER8 motifs are located within the XRE cluster, which is found to be critical for the AhR-mediated expression of both h*CYP1A1* and h*CYP1A2* (Ueda et al., 2006; Yoshinari et al., 2008), and one of the ER8 motifs (ER8$_1$) is found to be the CAR-responsive motif. In our previous study, CAR and AhR synergistically transactivated h*CYP1A1* and h*CYP1A2* expression (Yoshinari et al., 2010). In consistent with this, LXRα synergistically transactivated both genes with AhR. In contrast, LXRα and CAR did not show any synergistic effect on the transcription of h*CYP1A1* and h*CYP1A2*. This is probably because these two receptors share their binding motifs and have similar ability to transactivate both h*CYP1A1* and h*CYP1A2*, as shown in this study. Taken together, LXRα may function as a positive regulator of h*CYP1A1* and h*CYP1A2* expression independent of AhR but compete with CAR for the transcription of these genes.

During the course of our present experiments, Shibahara et al. reported that hLXRα transactivated h*CYP1A1* in HepG2 cells (Shibahara et al., 2011), which is consistent with our present results. Their results of chromatin immunoprecipitation assays indicate that the receptor binds to a region from −446 to −607 of h*CYP1A1* in response to LXRα agonist T0901317 (Shibahara et al., 2011). Consistently, two ER8 motifs found in our study are included within this region. It is thus strongly suggested that this region is critical